Environmental Pollution 316 (2023) 120688

Contents lists available at ScienceDirect

Environmental Pollution

journal homepage: www.elsevier.com/locate/envpol

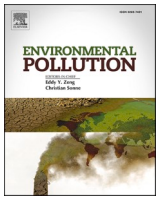

Consequences of *in vitro* benzyl butyl phthalate exposure for blubber gene expression and insulin-induced Akt activation in juvenile grey seals☆

Alexandra Tranganida [a,b], Ailsa J. Hall [a], Holly C. Armstrong [a,b,c], Simon E.W. Moss [a], Kimberley A. Bennett [b,*]

[a] Sea Mammal Research Unit, Scottish Oceans Institute, University of St Andrews, KY16 8LB, UK
[b] Division of Health Science, School of Applied Sciences, Abertay University, Dundee, DD1 1HG, UK
[c] School of Psychology and Neuroscience, University of St Andrews, KY16 9JP, UK

ARTICLE INFO

Keywords:
Adipose
Metabolic disruption
Endocrine disruption
Pinniped
Explant

ABSTRACT

Plastic and plasticiser pollution of marine environments is a growing concern. Although phthalates, one group of plasticisers, are rapidly metabolised by mammals, they are found ubiquitously in humans and have been linked with metabolic disorders and altered adipose function. Phthalates may also present a threat to marine mammals, which need to rapidly accumulate and mobilise their large fat depots. High molecular weight (HMW) phthalates may be most problematic because they can accumulate in adipose. We used blubber explants from juvenile grey seals to examine the effects of overnight exposure to the HMW, adipogenic phthalate, benzyl butyl phthalate (BBzP) on expression of key adipose-specific genes and on phosphorylation of Akt in response to insulin. We found substantial differences in transcript abundance of *Pparγ, Insig2, Fasn, Scd, Adipoq* and *Lep* between moult stages, when animals were also experiencing differing mass changes, and between tissue depths, which likely reflect differences in blubber function. Akt abundance was higher in inner compared to outer blubber, consistent with greater metabolic activity in adipose closer to muscle than skin, and its phosphorylation was stimulated by insulin. Transcript abundance of *Pparγ* and *Fasn* (and *Adipoq* in some animals) were increased by short term (30 min) insulin exposure. In addition, overnight *in vitro* BBzP exposure altered insulin-induced changes in *Pparγ* (and *Adipoq* in some animals) transcript abundance, in a tissue depth and moult stage-specific manner. Basal or insulin-induced Akt phosphorylation was not changed. BBzP thus acted rapidly on the transcript abundance of key adipose genes in an Akt-independent manner. Our data suggest phthalate exposure could alter seal blubber development or function, although the whole animal consequences of these changes are not yet understood. Knowledge of typical phthalate exposures and toxicokinetics would help to contextualise these findings in terms of phthalate-induced metabolic disruption risk and consequences for marine mammal health.

1. Introduction

Global contamination by plastics and the chemicals involved in their manufacture is a growing existential threat to biodiversity, as well as animal and human health (Landrigan et al., 2020; Persson et al., 2022). Plastic pollution is on course to double (Lebreton and Andrady, 2019; United Nations Environment Programme, 2021) and annual emissions may reach up to 53 million metric tonnes by 2030 (Borrelle et al., 2020). Of the plastic waste generated in 2016, 11%, or 19–23 million metric tonnes, was estimated to enter aquatic ecosystems (Borrelle et al., 2020), and the cumulative mass of ocean plastic waste is predicted to have increased from 2010 levels by an order of magnitude by 2025 (Jambeck et al., 2015). Phthalates are used to ensure plastic flexibility and durability (Daniels, 2009; Persico et al., 2009), but are not covalently bound to the material, migrate to its surface and can leach out to contaminate the environment (Navarro et al., 2010; Kastner et al., 2012). Phthalates can thus reach the marine environment not only through direct release into the atmosphere or waterways during plastic manufacture or disposal, but also through leaching from widespread plastic waste (World Health Organization & International Programme on Chemical Safety, 1999; Paluselli et al., 2019). Phthalates can account for 0.5–60% of plastic mass (Fromme, 2011), and leach out very slowly over months

☆ This paper has been recommended for acceptance by Maria Cristina Fossi.
* Corresponding author.
E-mail address: k.bennett@abertay.ac.uk (K.A. Bennett).

https://doi.org/10.1016/j.envpol.2022.120688
Received 1 August 2022; Received in revised form 27 October 2022; Accepted 15 November 2022
Available online 16 November 2022

to years (Paluselli et al., 2019), representing a potential major and long lasting source of pollution. Benzyl butyl phthalate (BBzP), one high molecular weight (HMW) phthalate was, until recently, produced in large volumes (Harris et al., 1997) for use in polyvinyl chloride (PVC) manufacture, which accounts for ~10% of global plastic demand (Plastics Europe, 2021). BBzP continues to be detected in wastewater, sea water, sediments and biota (Baini et al., 2017; Beltifa et al., 2017; Wang et al., 2021; Hidalgo-Serrano et al., 2022) and associated with marine microplastics (Omowunmi et al., 2020), despite a reduction its production and release. Phthalate pollution in the marine environment is therefore ubiquitous and will continue to be so, even under scenarios of reduced plastic use and better waste management (Lau et al., 2020).

The extended input of plastics into the marine environment and the contribution from contaminated landfill run-off suggest phthalates may pose a risk to a range of marine and coastal species, including marine mammals. While low molecular weight phthalates do not biomagnify though food chains (Mackintosh et al., 2004) and are typically easily excreted by mammals (Janjua et al., 2008; Koch et al., 2013), HMW phthalates have a higher octanol: water co-efficient (K_{ow}) and can accumulate in fat tissue (Mes et al., 1974; Fossi et al., 2012). Although direct plastic ingestion is thought to be low in most marine mammal species (Nelms et al., 2018; Senko et al., 2020), except for filter feeders, such as baleen whales (Fossi et al., 2012, 2014), there is evidence in pinnipeds of trophic transfer of microplastics (Nelms et al., 2019). In addition, the bioaccumulative and biomagnification potential of HMW phthalates (World Health Organization & International Programme on Chemical Safety, 1999; Beltifa et al., 2017) may mean top predators with large fat stores, such as pinnipeds, are exposed to phthalates through the food chain even without direct plastic ingestion. Most studies in marine species have investigated the concentration of phthalate metabolites (such as mono(2-ethylhexyl) phthalate (MEHP) and monoethyl phthalate (MEP)) in urine (Hart et al., 2020; Dziobak et al., 2021; Dziobak et al., 2022), which have been found in cetaceans (Fossi et al., 2012; Rian et al., 2020; Hart et al., 2020; Montoto- Martínez et al., 2021). However, recent studies have confirmed the presence of HMW phthalates (both parent compounds and their metabolites) in cetacean and polar bear blubber (Baini et al., 2017; Routti et al., 2021), including BBzP and its major metabolites (Baini et al., 2017). Although body burdens of BBzP have not been reported for marine mammals, levels of BBzP of 260–1629 ng g^{-1} dry weight have been recorded in skin and blubber biopsies from fin whales (*Balaenoptera physalus*) and Risso's dolphins (*Grampus griseus*) (Baini et al., 2017).

The half-life of phthalate metabolites is 6–18 h in humans (Janjua et al., 2008; Koch et al., 2013). Nevertheless, exposure is so pervasive that over 75% and up to 100% of the people sampled in population level studies have detectable levels in their urine (Koch et al., 2017; van der Meer et al., 2020). Epidemiological studies in humans, show moderately strong evidence of a link between phthalate doses below the tolerable daily intake (TDI) of 50 μg/kg/day (European Food Safety Authority, EFSA CEP Panel et al., 2019) and metabolic disorders, including diabetes, insulin resistance and obesity (Radke et al., 2019; van der Meer et al., 2020; Zhang et al., 2022). *In vitro*, phthalates can act as agonists of peroxisome proliferator-activated receptor gamma (PPARγ), a key regulator of glucose and lipid metabolism (Bility, 2004; Hurst and Waxman, 2003), and promote adipogenesis in pre-adipocytes (Feige et al., 2007; Pereira-Fernandes et al., 2013, 2014; Yin et al., 2016; Sakuma et al., 2017). Phthalates can also disturb adipocyte energy metabolism (Ellero-Simatos et al., 2011; Chiang et al., 2016) and induce or worsen insulin insensitivity in hepatocytes (Ding et al., 2019a). *In vivo* studies also show increased fat gain and/or perturbed fat metabolism in rodents (Jia et al., 2016; Moody et al., 2019a a,b) and in larval zebrafish (Guo et al., 2020) exposed to phthalates. Phthalates can act through phosphatidylinositol-3-kinase (PI3K)/ protein kinase B (Akt), a key effector in the insulin signalling pathway (Pereira-Fernandes et al., 2014; Mohammadi and Ashari, 2021). High doses in rodents can also reduce insulin secretion and exacerbate glucose intolerance and insulin insensitivity mediated by altered signalling through PI3K and Akt (Deng et al., 2018; Ding et al., 2019b; Mondal and Mukherjee, 2020; Mohammadi and Ashari, 2021). BBzP is a particularly obesogenic phthalate (Yin et al., 2016), more so than other, more abundant HMW phthalates, such as di(2- ethylhexyl) phthalate (DEHP) and diisononyl phthalate (DiNP) (Pereira-Fernandes et al., 2013, 2014).

Marine mammals are particularly vulnerable to chemicals that can disrupt lipid metabolism and energy balance due to their heavy reliance on lipid as a metabolic fuel (Reilly, 1991; Bennett et al., 2007); requirement for blubber as insulation (Irving and Hart, 1957); and strong links between adiposity and both first year survival (Hall et al., 2002) and adult reproductive fitness (Pomeroy et al., 1999; Lidgard et al., 2005). Disruption to insulin signalling and/or fat tissue function by local phthalate exposure may thus be detrimental to appropriate fat accumulation and mobilisation in marine mammals, especially during vulnerable life history phases. Seals appear to be relatively insensitive to insulin and glucose challenge during their natural, extended land-based fasting periods (Viscarra et al., 2011a, b; Olmstead et al., 2017). However, their insulin sensitivity is modulated, such that it falls throughout fasting, is less pronounced when animals are ashore moulting compared to breeding, and downstream elements, such as glucose transporter type 4 (GLUT4) and AMP-kinase, are not always downregulated (Houser et al., 2013). Although the involvement of insulin in energy balance in seals differs from terrestrial models, insulin is associated with mass gain in non-fasting states, such as in suckling pups and rehabilitated juveniles (Bennett et al., 2013, 2015; Fowler et al., 2020), suggesting sensitivity to this hormone may be important during weight gain phases and particularly for young animals.

Here we employed an explant approach (Bennett et al., 2017, 2021; Robinson et al., 2018) using blubber from juvenile grey seals (*Halichoerus grypus*) during periods of mass loss (moulting/recently moulted) and mass gain (post moult) to examine the effect of an overnight *ex vivo* exposure to micromolar concentrations of BBzP on insulin sensitivity and the expression of genes involved in fat metabolism. We used BBzP because it has a higher K_{ow} than low molecular weight phthalates, making it more lipophilic and thus likely to be more problematic for adipose tissue; because its recent high production volumes for PVC manufacture mean it continues to be identified in marine food webs (Beltifa et al., 2017), including in marine mammal blubber (Baini et al., 2017); and because it is typically reported as one of the most potent endocrine disrupting phthalates, with adipogenic and insulin signalling effects (Pereira-Fernandes et al., 2013, 2014; Yin et al., 2016; Sakuma et al., 2017; Zhang and Choudhury, 2021). We investigated the transcription factor *Pparγ,* and genes involved in lipogenesis (Stearoyl-CoA Desaturase (*Scd)*), cholesterol metabolism (Insulin Induced Gene 2 (*Insig2)*), fatty acid synthesis (*Fasn*), and the adipokine energy regulators adiponectin and leptin. BBzP had no effect on activation of the canonical insulin signalling cascade through Akt, but caused tissue depth-specific changes to transcript abundance of *Pparγ* that also depended on moult stage or mass change trajectory. These data suggest phthalates can alter insulin-induced gene transcription changes in seals through Akt-independent pathways, but the longer-lasting and whole animal consequences of such alterations remain unclear.

2. Materials and methods

Ethical approval

Animal capture and sample collection were performed under the Sea Mammal Research Unit (SMRU) Animal (Scientific Procedures) Act, 1986 (ASPA) Home Office Project Licence (70/7806, digital identifier: 192CBD9F) and associated personal licences. This work received ethical approval from Abertay University and the University of St Andrews Animal Welfare and Ethics Committee (AWEC) and was performed in compliance with ASPA and the EU Directive on the Protection of Animals used for Scientific Purposes (2010/63/EU).

2.1. Animal capture and husbandry

Field work was conducted in the Moray Firth, Scotland, during May through August 2018. Seven wild, juvenile moulting or recently moulted grey seals were captured using seine nets and handheld hoop nets and transported (in accordance with the SMRU Project Licence) under sedation (a mass-specific intramuscular dose of 0.5–1.0 mg kg^{-1} midazolam (5 mg ml^{-1}, Hypnovel, Roche, Welwyn Garden City, UK)) to the SMRU Home Office Licenced captive seal facility, where they remained for a maximum of seven months before their release back into the wild. While in captivity, animals' health was assessed daily. They were fed every day with 2.8 ± 1.2 kg of herring (occasionally sprat, hake, or sandeel) (Marine Nutrition, Grimsby, England) supplemented with vitamins (1 Aquavits and 300 mg ferrous gluconate per day, supplied by the International Zoo Veterinary Group). Monthly seawater quality assessments were carried out by a United Kingdom Accreditation Service (UKAS) approved laboratory (Tayside Scientific Services, Dundee).

2.2. Biopsy sampling

Sedation and anaesthesia included a mass specific intravenous dose of Zoletil® 100 for general anaesthesia and subcutaneous Lignol®. Three 10 mm and one 6 mm blubber biopsies were taken from each animal. The 10 mm biopsies were used for the generation of explants as described previously (Bennett et al., 2017; Robinson et al., 2018, 2021) and the 6 mm biopsy was used for measurement of lipid percentage (Robinson et al., 2019). Tissue was cut immediately, using sterile surgical scissors, into inner (blubber layer closest to the muscle) and outer (blubber layer closest to the skin) sections, and placed into separate 15 mL centrifuge tubes filled with sterile Krebs Ringer solution (37 °C, pH 7.4; NaCl; 7.89 g L^{-1}; KCl; 0.373 g L^{-1}; $MgSO_4$; 0.12 g L^{-1}; K_2HPO_4; 0.07 g L^{-1}; glucose; 0.99 g L^{-1}; 4-(2-hydroxyethyl)-1-piperazineethanesulfonic acid (HEPES); 4.77 g L^{-1}; $CaCl_2$; 0.11 g L^{-1}) with 1% Antibiotic Antimycotic Solution (all chemicals supplied by Sigma Aldrich, Gillingham, UK) for transport back to the laboratory. A single hidden suture (Ethicon Vicryl Suture (W9114) Violet, 3−0, 20 mm, 75 cm with VICRYL Suture 1/2 circle "Taper Point Plus" Needle) was used to close the biopsy sites. The animals were kept at the SMRU pool facility until they had fully healed and finished their moult, when a second set of samples was collected following the same procedure.

3. Lipid ecpercentage

Lipid percentage was determined gravimetrically after solvent evaporation using 200 mg of blubber from the 6 mm biopsy as described in Robinson et al. (2019).

3.1. Explant culture and phthalate exposure

The 10 mm blubber biopsies were washed with warm Krebs Ringer buffer and visible hair, muscle, and blood contaminated tissue was removed. The tissue was then minced using sterile scalpels and 100 mg explants were transferred into prepared 12-well plates and incubated for a total of 24 h in a humidified chamber (37 °C, 5% CO_2). Similar to experiments described previously for Aroclor exposure (Robinson et al., 2018), 1500 μL of either complete cell culture media (medium 199, Hanks' Balanced Salts with 1% Antibiotic Antimycotic Solution, 1% fatty acid supplement and 5% charcoal stripped fetal bovine serum) or complete media containing 10 μM BBzP (chemicals supplied by Sigma Aldrich), was added per well to generate control and BBzP treatments. This dose of BBzP is 10 fold below toxicity levels in cell viability assays on preadipocytes and induces fat accumulation, adipogenic gene expression and altered metabolic characteristics (Yin et al., 2016; Pereira-Fernandes et al., 2014). After 23.5 h incubation, 150 μL media were removed and then replaced with 150 μL of fresh control media or media containing insulin at a final dose of 30 ng mL^{-1} for an additional 30-min. After insulin incubation, media was removed and frozen at −80 °C, and explants were flash frozen in liquid nitrogen and stored at −80 °C until further use.

3.2. Total RNA and protein isolation

Total RNA and protein were isolated from 100 mg tissue explants using TRIzol® Reagent (Invitrogen, Paisley, UK), with appropriate modifications for fatty tissue extraction, according to the manufacturers' instructions (Chomczynski and Mackey, 1995; Merck, 2022) as follows:

The explants were homogenised in 1 mL TRIzol using sterile micropestles. The homogenised tissue-TRIzol mixture was left at room temperature for 5 min to dissolve cell components, after which 100 μL of bromochloropropane (BCP) (Sigma Aldrich) were added. Samples were vortexed for 15 s, incubated at room temperature for 8 min, and then centrifuged for 15 min (4 °C, 11,500×*g*) using a benchtop centrifuge. The phenol phase was kept on ice for subsequent protein extraction.

3.3. Total RNA extraction

The aqueous phase containing RNA was collected and treated again with 100 μL BCP. The resulting aqueous phase was collected and 500 μL cold isopropanol (Thermo Fisher, Loughborough, UK) were added and mixed by inversion. Samples were incubated at −20 °C for 1 h and 20 min. Samples were then incubated at room temperature for 10 min and centrifuged at 12,000×*g* for 15 min at 4 °C. The supernatant was discarded, and the RNA pellet was washed three times with 500 μL cold 70% ethanol. The RNA pellet was air-dried and re-suspended in 15–20 μL molecular grade water (Invitrogen) and stored at −80 °C.

The concentration and purity of RNA were measured using a NanoDrop 2000 spectrophotometer (Thermo Scientific, Basingstoke, UK). Integrity was determined by gel electrophoresis as follows: 100–500 ng of total RNA mixed with 1X gel loading dye (Thermo Scientific) were separated on a 1% agarose gel, stained with SYBR® Safe DNA gel stain (Invitrogen) according to the manufacturer's protocol (Thermofisher.com, 2016a) The 28S and 18S ribosomal bands were visualised with a 1 Kb DNA ladder (Thermo Scientific) and examined for degradation. Samples with clear bands at 28S and 18S and no smearing were used in complementary DNA (cDNA) synthesis and analysis.

3.4. Protein isolation

Molecular grade ethanol (100%; 300 μL) was added to the phenol phase that was extracted from the TRizol-BCP treatment detailed above, (Chomczynski, 1993; Xiong et al., 2011). Samples were mixed by immersion and left at room temperature for 2 min before centrifugation for 5 min (4 °C, 2000 x g). The resulting supernatant was transferred to a clean tube containing 1500 μL isopropanol. Samples were incubated at room temperature for 10 min and then centrifuged (12,000×*g*) for 10 min. The supernatant was discarded, and the resulting protein pellet was washed three times with 2 mL 0.3 M guanidine hydrochloride in 95% ethanol solution followed by a final wash with 2 mL 100% ethanol. Ethanol was discarded and the protein pellet air dried. Pellets were dissolved in 50–150 μL of 1% sodium dodecyl sulphate (SDS) solution on a 50 °C heat block for 30 min. The volume used depended on pellet size. Protein extracts were stored at −80 °C.

A Pierce™ bicinchoninic (BCA) Protein Assay Kit (Thermo Scientific) was used to quantify total protein according to the manufacturers' instructions (Thermofisher.com, 2016b). Diluted extracts were assayed in duplicate in a 96-well plate format following the manufacturer's instructions, and measurement was collected in a BioTek ELx800 (Swindon, UK) plate reader at 550 nm.

3.5. mRNA transcript abundance

Expression of *Pparγ, Insig2, Fasn, Scd, Adipoq* and *Lep* was measured

by absolute qPCR using 7-point standard curves of the respective isolated amplicon as follows:

Prior to cDNA synthesis RNA was treated with DNAse (Roche) to eliminate genomic DNA (gDNA) contamination. cDNA was synthesised from 300 ng total RNA in a 20 μL reaction according to the manufacture's protocol (qPCRBIO cDNA Synthesis Kit; PCR Biosystems Ltd., London, UK). cDNA was diluted 1:10 and 4 μL were used per 10 μL qPCR reaction with qPCRBIO SyGreen Blue mix Hi-ROX (PCR Biosystems Ltd.).

A cDNA pool was used for the generation of amplicons for the construction of standard curves (PCR: 2 min at 95 °C; 30 cycles of 30 s at 95 °C, 30 sec 55 °C, 1 min at 72 °C and final extension of 10 min at 72 °C). Amplicons were visualised on a 1% agarose gel in Tris-borate-EDTA (TBE) (1X) buffer. The bands were visualised and excised on a UV-transilluminator using a sterile razor blade. Amplicons were extracted (QIAEX II Gel Extraction Kit, QIAGEN, Manchester, UK), following the manufacturer's instructions. The purified DNA was quantified using the Qubit® 3.0 Fluorometer (Invitrogen) and the Qubit HS dsDNA Assay kit (Invitrogen). Serial dilutions were performed on the purified DNA and were used to construct a seven-point standard curve in qPCR (Leong et al., 2007). Samples and controls were run in triplicate on a Mx3000P qPCR System (Agilent Technologies, Inc., Stockport, Cheshire, UK) (amplification program: 30 s at 95 °C, 35 cycles of 10 s at 95 °C and 30 s at 60 °C). Copy number was derived from the standard curve, in which the value on the y axis is plotted against $\log_{10}$ copy number and the linear equation derived: $y = mx + c$. The equation is rearranged and solved for the corresponding Ct value from the unknown sample (Leong et al., 2007). The value was anti-logged to give the absolute copy number of the unknown sample.

Information on primers used are in Table 1. All primers were used at 500 nM final concentration. *Pparγ, Adipoq* and *Lep* primers have been previously optimised and used with grey seal samples (Bennett et al., 2017). *Scd* primers were designed using Primer3 (Koressaar and Remm, 2007; Untergasser et al., 2012) against grey seal sequence (accession number: XP_035921000) available through the National Center for Biotechnology Information (NCBI). Primer specificity was evaluated by BLAST and confirmed by the amplification of a single product of the desired size on gel electrophoresis and by the presence of a single peak in melt curve analysis. The absence of primer-dimer formation and contamination was confirmed by the lack of amplification in no-template controls. Primer efficiency was calculated using standard curves of serially diluted pooled cDNA (Bustin and Huggett, 2017). Efficiencies of primers were between 85 and 110% and R^2 values for amplicon standard curves run on each plate were >0.99.

Table 1
Primer pairs used for qPCR.

Gene	Primer sequence	Applicon size (bp)	Efficiency (%)	Supplier
Pparγ	F: TCCAGCATTTCCACTCCACA R: GCAGGCTCCACTTGGATTGC	82	108.36	EUROFINS GENOMICS
Adipoq	F: TATGATGGCACCACTGGAAA R: GCCTGGTCCACATTCTTCTC	164	93.38	EUROFINS GENOMICS
Lep	F: CCCATCCAAAGAGTTCAGGA R: TAGACCAGCAACCCTTGGTC	74	95.50	EUROFINS GENOMICS
Insig2	F: AATCATGCCAGCGCTAAAGT R: TCAAAGGTCCACCAGAGTCC	79	99.05	IDT
Scd	F: GCTCTTCCTGATCCTTGCCA R: CTTTGACGGCTGGGTGTTTG	179	88.90	Invitrogen
Fasn	F: GGTGGACTCCCTGAAGAACG R: GAGACAGTTCACCATGCCCA	107	109.00	EUROFINS GENOMICS

3.6. Protein expression

Total protein (4 μg per well) was loaded in 4–10% Bis-Tris midi gels for electrophoretic separation (100 V, 1 h 20 min), based on prior optimisation to achieve a loading amount that lay on the linear portion of the curve of band density plotted against protein loaded. Prior to electrophoresis, samples were reduced with DL-dithiothreitol (Sigma Aldrich) on a heat-block (80 °C, 10 min). Novex Sharp pre-stained protein standard (Invitrogen) and MagicMark XP Western Protein Standard (Invitrogen) were used for molecular weight sizing. A protein pool sample was run on each gel and used to normalise samples to account for between gel variability (Bass et al., 2017).

Protein gels were blotted on polyvinylidene fluoride (PVDF) membranes (Invitrogen) using the iBlot™ 2 Gel Transfer Device (Invitrogen). Membranes were stained in Ponceau S solution (Sigma Aldrich) to check successful protein transfer. Membranes were de-stained in deionised water and blocked with gentle agitation in 5% bovine serum albumin (BSA) in Tris-Buffered Saline with Tween-20 (TBST) solution overnight at 4 °C.

3.7. Antibody incubation and chemiluminescent detection

Membranes were incubated for 1.5 h with gentle agitation at room temperature in blocking buffer containing one of the following primary antibodies (1:2000 dilution): Akt mouse monoclonal Antibody (2920S, Cell Signalling Technology, Leiden, The Netherlands), p-Akt (T308) rabbit monoclonal Ab (13,038, Cell Signalling Technology), p-Akt (S473) rabbit monoclonal Ab (4060S, Cell Signalling Technology). Blots were washed four times with TBST, prior to incubation in secondary antibody for 1 h with gentle agitation at room temperature. Secondary antibodies were supplied by Thermo Scientific and used in a 1:5000 dilution in 1% BSA in TBST. Washes were repeated and membranes were incubated in enhanced chemiluminescent (ECL) horseradish peroxidase (HRP) substrate (SuperSignalTM West Pico PLUS; Thermo Scientific) for 5 min for chemiluminescent detection. Membranes were imaged on a ChemiDoc™ XRS imager (Bio-rad) exposed for 1–120 s. Densitometric analysis of acquired images was performed using the GeneTools software (SYNGENE), using automatic lane and band detection and automatic background check. Phospho-Akt band volume values were normalised against total Akt of the respective sample (Bass et al., 2016).

3.8. Statistical analysis

Data were analysed in R (4.1.2) (R Core Team, 2021). Distribution of response variables was explored visually using histograms and was confirmed by Shapiro–Wilk tests. Where data did not have a normal distribution, either square root or log transformation was undertaken, and the transformation chosen based on the normalisation of residuals. *Pparγ* and *Insig2* were not transformed prior to analysis; *Fasn*, *Scd*, *Adipoq* and *Lep* copy number and total Akt abundance were square root transformed. Both relative abundance of p-Akt S473 and p-Akt T308 were log transformed. In each case, outliers were identified by boxplots and confirmed by Grubbs test, and significant outliers ($p < 0.05$) were removed from the dataset and the analysis repeated. Linear mixed effect models (LME) constructed using the *nlme* package in R (Pinheiro et al. 2018) with fixed intercepts were used to investigate the associations between variables. Animal identification (ID) was included as a random effect to account for repeated measurements from the same individual. Sex, sampling occasion, tissue depth (inner, outer) and treatment (control, insulin-treated, BBzP-treated, BBzP + insulin treated) were included as candidate variables that explain the variability in mRNA and

protein abundance. Co-linearity between explanatory variables was tested for each global model by calculating variance inflation factor (VIF) using the *car* package in R (Fox and Weisberg, 2011), and only variables with VIF <3 were included in each model (Zuur et al., 2010). Backwards model selection from the full model, which was selected based on plausible biological interactions between the explanatory variables, was then performed using the dredge function in *MuMIn* (Barton, 2018). The candidate models identified by dredge, for which ΔAICc was <2, were then assessed for model fit using residual and Q-Q plots. When more than one model was identified by dredge, residual distribution, model weights and importance and confidence intervals of explanatory variables of each model was compared and results from the best model overall were reported. Conditional and marginal R^2 were calculated for the selected models using the *piecewiseSEM* package in R (Lefcheck, 2016).

4. Results

4.1. Morphometric characteristics

Characteristics of study animals at each sampling occasion are summarised in Table 1SI. Animals lost mass after the first sample but were gaining mass when the second sample was collected. Total body mass and blubber lipid percentage were higher in the second sample (mass: paired *t*-test: t (13) = 22.74, p < 0.001, 95% CI [−51.11, −42.24]; lipid percentage: paired *t*-test: t (13) = 17.53, p < 0.001, 95% CI [−72.21, −56.36]) (Fig. 1SI). Mass increased by 10.46 kg (min. 3.4, max. 21 kg) and lipid percentage increased 25.9% (min. 15, max. 36%). Males and females did not differ in percentage lipid content in either first (Mann-Whitney *U* test: W = 5, p = 0.3725) or second sample (Mann-Whitney *U* test: W = 5, p = 0.8571).

4.2. Gene expression

4.2.1. Pparγ, Insig2, Fasn, Scd

The top models (ΔAICc <2) that best explain the variance for each target gene and protein are summarised in Table 2SI. Models selected for the final analysis are summarised in Table 2.

4.2.2. Pparγ

Pparγ copy number changed between first and second sampling, and the pattern of change differed by tissue depth and sex (LME: $R^2_{marginal}$ = 0.24; $R^2_{conditional}$ = 0.48; $n_{observations}$ = 91; $n_{animals}$ = 6). Depth differences in *Pparγ* copy number were not apparent in the first sample, but became apparent in the second sample when outer had higher copy number than inner in each sex. The pattern of change was sex specific: in females, *Pparγ* copy number was lower in the second sample in inner tissue (t (75) = 4.25, p < 0.001, 85% CI [−131.04, −64.21]), whereas in males, *Pparγ* copy number was higher in the second sample in outer tissue (t (75) = 3.07, p = 0.003, 85% CI [38.56, 107.82]) (Fig. 1A).

Pparγ copy number was significantly higher in inner compared to outer tissue in the first sampling in the control (t (75) = 2.40, p = 0.019, 85%CI [−113.84, −27.86]) and insulin treated explants (t (75) = −2.31, p = 0.0238, 85% CI [−112.24, −25.46]), but not in BBzP explants, suggesting BBzP minimised basal and insulin-induced depth differences in *Pparγ* expression when animals were moulting and losing weight. In the second sample, *Pparγ* copy number was significantly higher in outer compared to inner tissue in BBzP (t (75) = 2.25, p = 0.027, 85% CI [23.57, 109.55]) and BBzP + insulin explants (t (75) = 4.77, p < 0.001, 85% CI [104.65, 196.36]), suggesting BBzP enhanced the depth differences when animals were post moult and gaining weight.

Inner-outer differences may be due to divergent responses to insulin treatment. In inner tissue, the insulin treated group had significantly higher *Pparγ* mRNA content compared to the BBzP (t (75) = 2.12, p = 0.040, 85% CI [−93.87, −17.43]) and BBzP + insulin explants (t (75) = 2.63, p = 0.011, 85% CI [−109.86, −31.53]), suggesting suppression of insulin action by BBzP. The effects of the treatments were not the same in outer tissue: insulin treatment and BBzP treatment alone did not affect *Pparγ* copy number compared to controls. However, the *Pparγ* copy number in BBzP + insulin treated explants was significantly higher compared to control (t (75) = 2.38, p = 0.020, 85% CI [−109.78, −26.54]) and BBzP treated explants (t (75) = 2.41, p = 0.019, 85% CI [−110.53, −27.29]), but no different from the insulin treated explants (t (75) = 1.57, p = 0.121, 85% CI [−88.63, −3.35]). In outer tissue, BBzP treatment thus seemed to enhance the insulin effect, which contrasts with the suppressive effect in inner tissue (Fig. 1B).

4.2.3. Fasn

Sampling occasion, tissue depth, sex, treatment and some of their interactions best explained *Fasn* copy number variance (Table 2) (LME: $R^2_{marginal}$ = 0.18, $R^2_{conditional}$ = 0.57; $n_{observations}$ = 86; $n_{animals}$ = 6). *Fasn* copy number was significantly higher in inner compared to outer tissue in both sexes in the first sample (females: t (72) = 4.59, p < 0.001, 85% CI [−4.07, −2.11]; males: t (72) = 2.77, p = 0.007, 85% CI [−2.85, −0.89]). This depth difference was not seen in the second sample (females: t (72) = −1.39, p = 0.169, 85% CI [−1.86, 0.04]; males: t (72) = 0.49, p = 0.63, 85% CI [−0.62, 1.24]) and the changes were sex-specific. In females, *Fasn* copy number was higher in the second compared to first sample in outer tissue (t (72) = 3.80, p < 0.001, 85% CI [1.59, 3.56]). In males, *Fasn* copy number was significantly higher in the first compared to second sample in inner tissue (t (72) = 2.36, p = 0.02, 85% CI [−2.45, −0.58]). Insulin treated explants had significantly higher *Fasn* copy number compared to control (t (72) = 2.40, p = 0.019, 85% CI [−2.05, −0.50]) and BBzP treated explants (t (72) = 2.04, p = 0.045, 85% CI [−1.87, −0.31]), but not compared to insulin + BBzP treated explants, suggesting that BBzP did not impact the insulin effect on *Fasn* copy number (Fig. 2).

4.2.4. Insig2

Sampling occasion, depth and their interaction were the best explanatory variables for *Insig2* copy number (LME: $R^2_{marginal}$ = 0.133, $R^2_{conditional}$ = 0.203; $n_{observations}$ = 90; $n_{animals}$ = 6). *Insig2* copy number decreased from first to second sampling (t (81) = 3.20, p < 0.001, 85% CI [−25.63, −9.62]) in inner tissue, and increased in outer tissue over the same period (t (81) = 2.04, p = 0.044, 85% CI [3.40, 20.15]). Copy number was higher in inner compared to outer tissue in the first

Table 2
Best fitted LME models for drivers of Pparγ, Insig2, Fasn, Scd, Adipoq, and Lep copy number, and total Akt, p-S473 and p-T308 expression. Df = degrees of freedom.

Gene	Model	Explanatory variables (* indicates interaction)	Df	AICc
Pparγ	1	sampling occasion, depth, sex, treatment, sampling occasion*depth, sampling occasion*sex, depth*treatment	14	1049.07
Insig2	1	sampling occasion, depth, sampling occasion*depth	6	798.06
Fasn	6	sampling occasion, depth, sex, treatment, sampling occasion*depth, sampling occasion*sex, depth*sex	12	372.99
Scd	1	sampling occasion, depth, sampling occasion*depth	6	962.44
Adipoq	3	Sampling occasion, depth, sex, sampling occasion*sex	7	813.87
Lep	1	Sampling occasion, depth, sex, sampling occasion*depth, sampling occasion*sex	8	560.70
Total Akt	2	sampling occasion, depth, sex, sampling occasion*depth, sampling occasion*sex	8	52.3
p-Ser473	1	sampling occasion, depth, treatment, sampling occasion*depth	9	305.58
p-Thr308	1	Sampling occasion, depth, sex, treatment, sampling occasion*sex	10	277.3

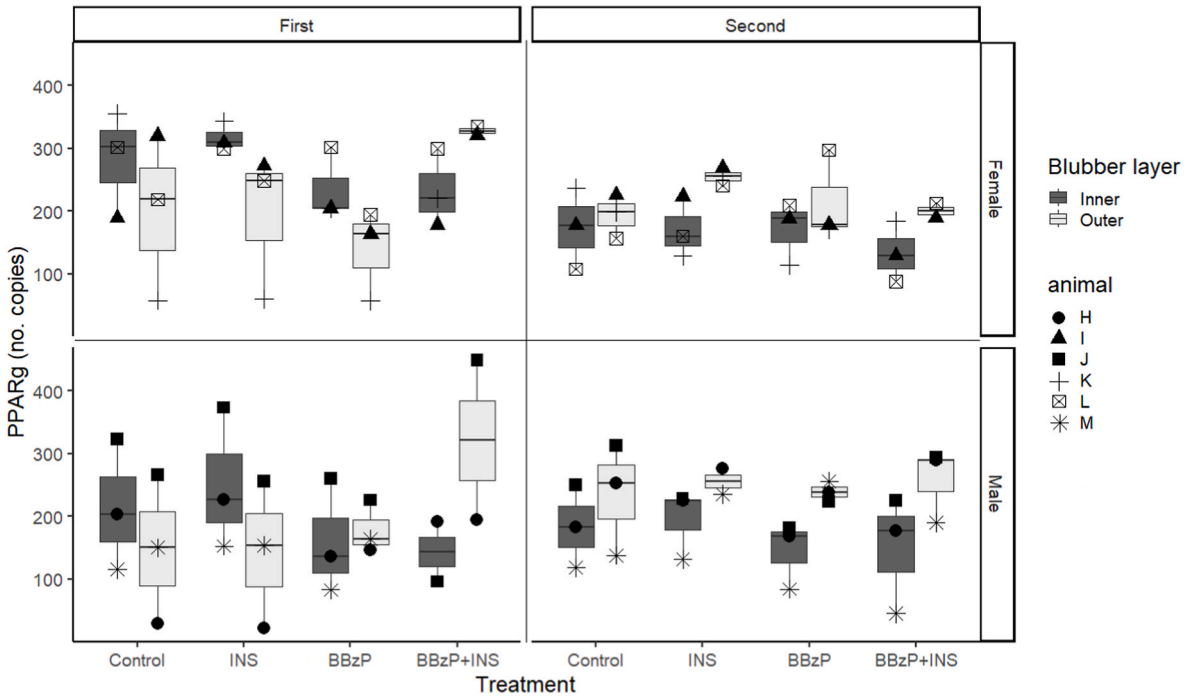

Fig. 1. *Pparγ* copy number vs treatment in inner and outer tissue on the two sampling occasions (left: first sample; right: second sample) in females (top panels) and males (bottom panels). Boxplots with upper and lower quartiles and 1.5 × interquartile range. Each point represents an observation ($n_{observations} = 91$; $n_{animals} = 6$).

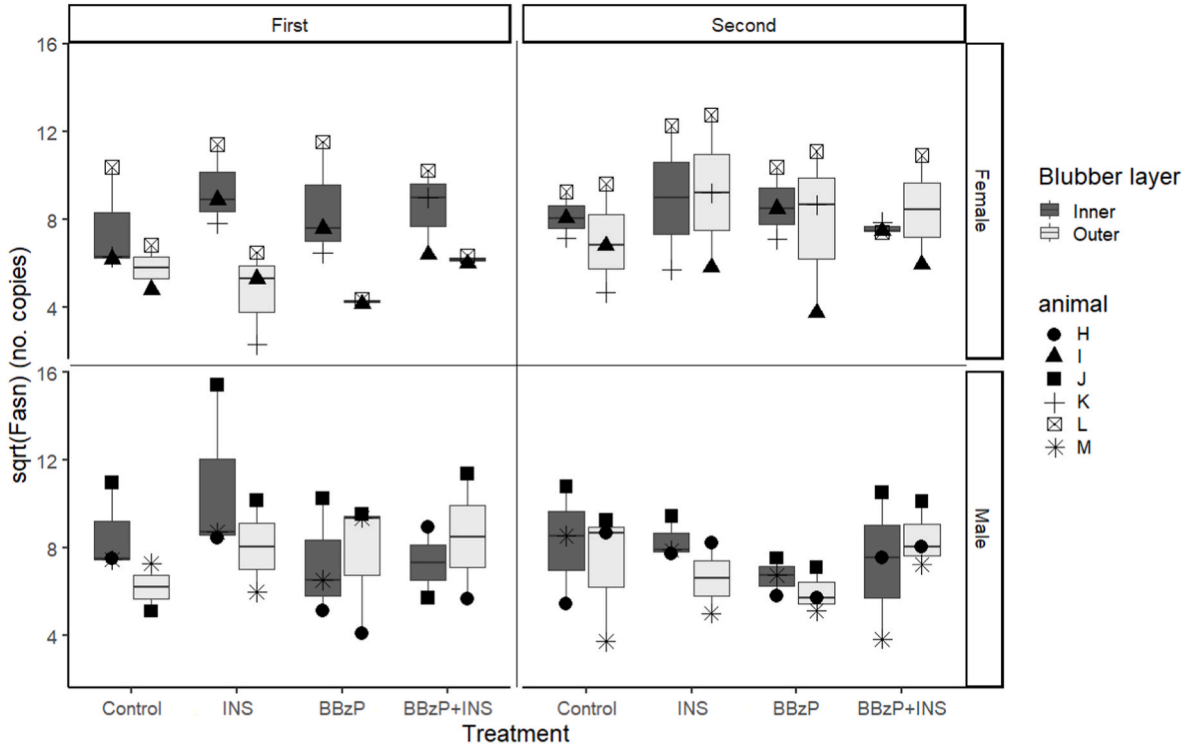

Fig. 2. sqrt (*Fasn*) copy number vs treatment in inner and outer tissue, on the two sampling occasions (left: first sample; right: second sample) in females (top panels) and males (bottom panels). Boxplots with upper and lower quartiles and 1.5 × interquartile range. Each point represents an observation ($n_{observations} = 86$; $n_{animals} = 6$).

sampling (t (81) = 3.062, $p < 0.001$, 85% CI [−25.76, −9.18]) and the opposite was true in the second sampling (t (81) = 2.14, p = 0.035, 85% CI [3.84, 20.03]) (Fig. 3A). Neither insulin treatment nor BBzP altered *Insig2* copy number.

4.2.5. *Scd*

Sampling occasion, depth and their interaction were the selected explanatory variables in the best fitted model (LME: $R^2_{marginal}$: 0.175, $R^2_{conditional} = 0.467$; $n_{observations} = 91$, $n_{animals} = 6$). In the second sample, outer tissue had significantly higher *Scd* copy number compared to inner

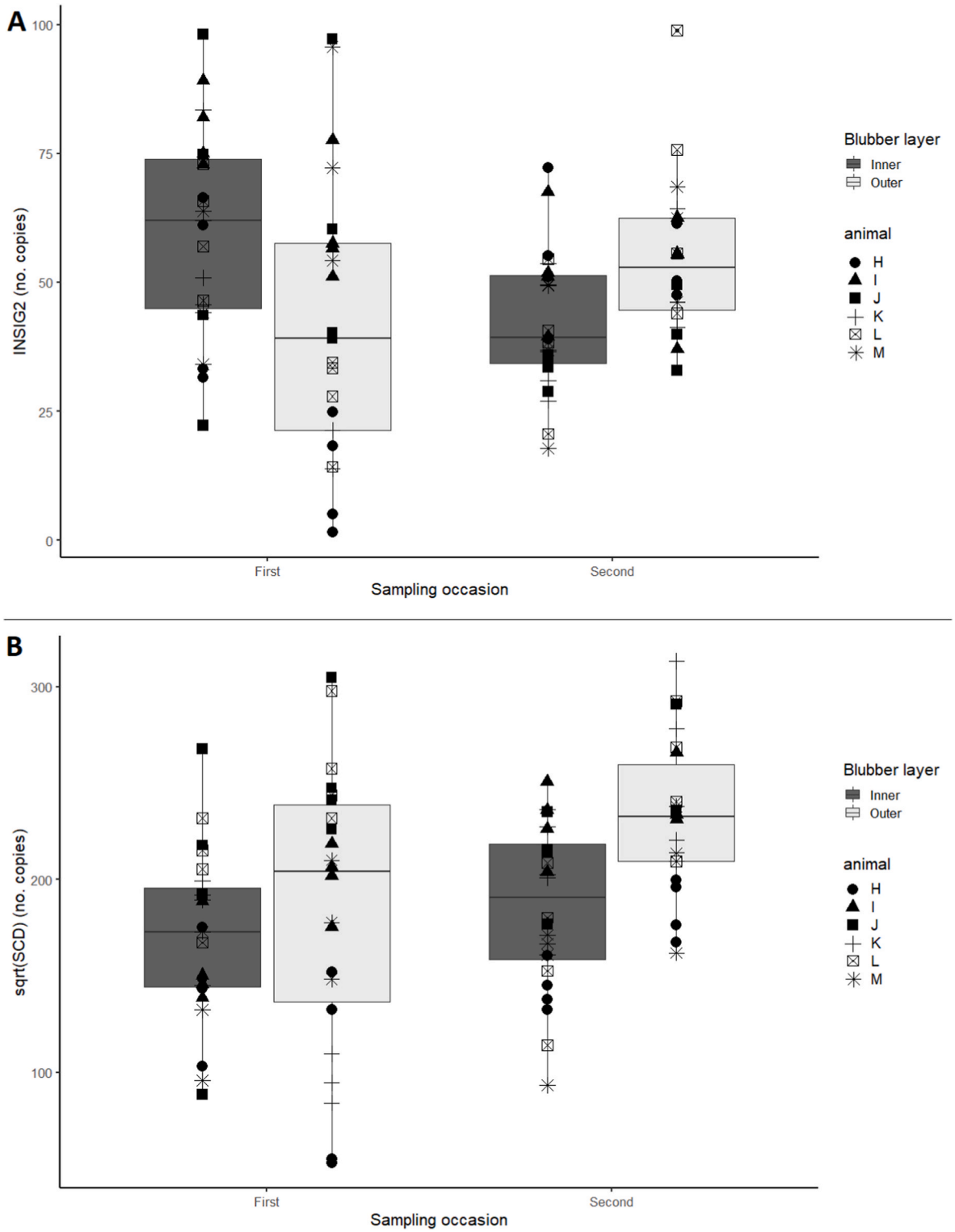

Fig. 3. (A) *Insig2* copy number in inner and outer blubber layers on the two sampling occasions, with upper and lower quartiles and 1.5 × interquartile range. Each point represents an observation ($n_{observations} = 90$; $n_{animals} = 6$). (B) sqrt (*Scd*) copy number in inner and outer tissue on the two sampling occasions. Boxplots with upper and lower quartiles and 1.5 × interquartile range. Each point represents an observation ($n_{observations} = 91$, $n_{animals} = 6$).

(t (82) = 3.86, p < 0.001, 85% CI [30.15, 66.55]). This inner-outer difference was likely driven by an increase in the second sampling in outer tissue (t (82) = 3.89, p < 0.001, 85% CI [31.17, 68.38]) in some, but not all, animals (Fig. 3B).

4.3. Adipokine transcript abundance: leptin and adiponectin

4.3.1. Adipoq

The model with the best residual distribution retained sampling occasion, depth, sex and the interaction between sampling occasion and sex as explanatory variables (LME: marginal $R^2_{LME} = 0.33$; conditional

R^2_{LME} = 0.48; $n_{observations}$ = 91; $n_{animals}$ = 6). Irrespective of sex and sampling occasion, copy number was significantly higher in outer compared to inner tissue (t (82) = 2.31, p = 0.024, 85% CI [3.40, 14.99]). In both sexes, *Adipoq* copy number was lower in the second sample (females: t (82) = 6.19, p < 0.001, 85% CI [−42.80, −26.53]; males: t (82) = 3.23, p = 0.002, 85% CI [−26.60, −10.10]).

In this model, some observations (denoted with arrows in Fig. 4) in outer tissue were identified as influential points in residual plots using Cook's distance, and the model selection was repeated after their removal from the dataset. Only one model was selected after data removal (ΔAICc <2) and it retained the same variables as before, with the addition of treatment (LME: $R^2_{marginal}$ = 0.61; $R^2_{conditional}$ = 0.78; $n_{observations}$ = 86; $n_{animals}$ = 6). As in the previous model, copy number decreased from first to second sample in both sexes (females: t (74) = 11.58, p < 0.001, 85% CI [−48.65, −37.79]; males: t (74) = 6.58, p < 0.001, 85% CI [−29.94, −19.10]) and was significantly higher in outer compared to inner blubber layer (t (74) = 6.58, p < 0.001, 85% CI [13.61, 21.34]). In addition, copy number in the insulin treated explants was significantly higher compared to the BBzP and BBzP + insulin treated explants (BBzP: t (74) = 2.86, p = 0.006, 85% CI [−15.78, −5.14]; BBzP + insulin: t (74) = 2.46, p = 0.016, 85% CI [−14.91, −3.83]) but not compared to the control (t (74) = 1.02, p = 0.312, 85% CI [−9.14, 1.61]) (Fig. 4B).

4.3.2. Lep

The best model retained sampling occasion, depth, sex and some of their interactions as explanatory variables, and the majority of the variance was explained by the random effect (LME: $R^2_{marginal}$ = 0.15; $R^2_{conditional}$ = 0.54; $n_{observations}$ = 91; $n_{animals}$ = 6). In the second sample inner *Lep* copy number was significantly lower compared to outer (t (81) = 2.79, p = 0.007, 85% CI [1.79, 5.69]). In males, outer tissue had significantly lower *Lep* copy number in the first compared to the second sample (t (81) = 5.05, p < 0.001, CI 85% [6.02, 10.88]) (Fig. 5). There were no effects of insulin or BBzP.

4.4. Protein abundance data

4.4.1. Total Akt abundance

Sampling occasion, tissue depth, sex and interactions best explained the variance in total Akt band density (LME: $R^2_{marginal}$ = 0.17; $R^2_{conditional}$ = 0.48; $n_{observations}$ = 109; $n_{animals}$ = 7). Regardless of sex, total Akt content was significantly higher in inner tissue (first sampling: t (98) = 4.93, p < 0.001, 85% CI [−0.48, −0.26]; second sampling: t (98) = 1.99, p = 0.050, 85% CI [−0.25, −0.04]). In females, outer tissue Akt content was significantly higher in the second sample (t (98) = 3.29, p = 0.001, 85% CI [0.18, 0.45]) (Fig. 6A).

4.4.2. p-S473

The model that best explained p-S473 variance retained sampling occasion, blubber depth, treatment, and the interaction between sampling occasion and depth as the explanatory variables (LME: marginal R^2_{LME} = 0.47; conditional R^2_{LME} = 0.59; $n_{observations}$ = 108; $n_{animals}$ = 7). Insulin treatment significantly increased p-S473 content compared to controls (t (95) = 7.17, p < 0.0001, 85% CI [−2.05, −1.36]) and BBzP treated group (t (95) = 7.47, p < 0.0001, 85% CI [−2.12, −1.43]). BBzP treatment did not influence p-S473 content (t (95) = 0.30, p = 0.76, 85% CI [−0.27, 0.42]). BBzP also did not affect the insulin effect in the combined treatment group (t (95) = 0.50, p = 0.62, 85% CI [−0.24, 0.49]) (Fig. 6C). p-S473 content was higher in outer compared to inner tissue in the second sample (t (95) = 3.43, p < 0.001, 85% CI [0.48, 1.17]), while no tissue depth difference was observed in the first sample (t (95) = 0.11, p = 0.92, 85% CI [−0.38, 0.33]) (Fig. 6B).

4.4.3. p-T308

Sampling occasion, blubber depth, sex, treatment and sampling occasion-sex interaction were retained as explanatory variables (LME: marginal R^2_{LME} = 0.68; conditional R^2_{LME} = 0.72; $n_{observations}$ = 108; $n_{animals}$ = 7). Insulin treatment significantly increased p-T308 content compared to controls (t (95) = 11.06, p < 0.001, 85% CI [−2.64,

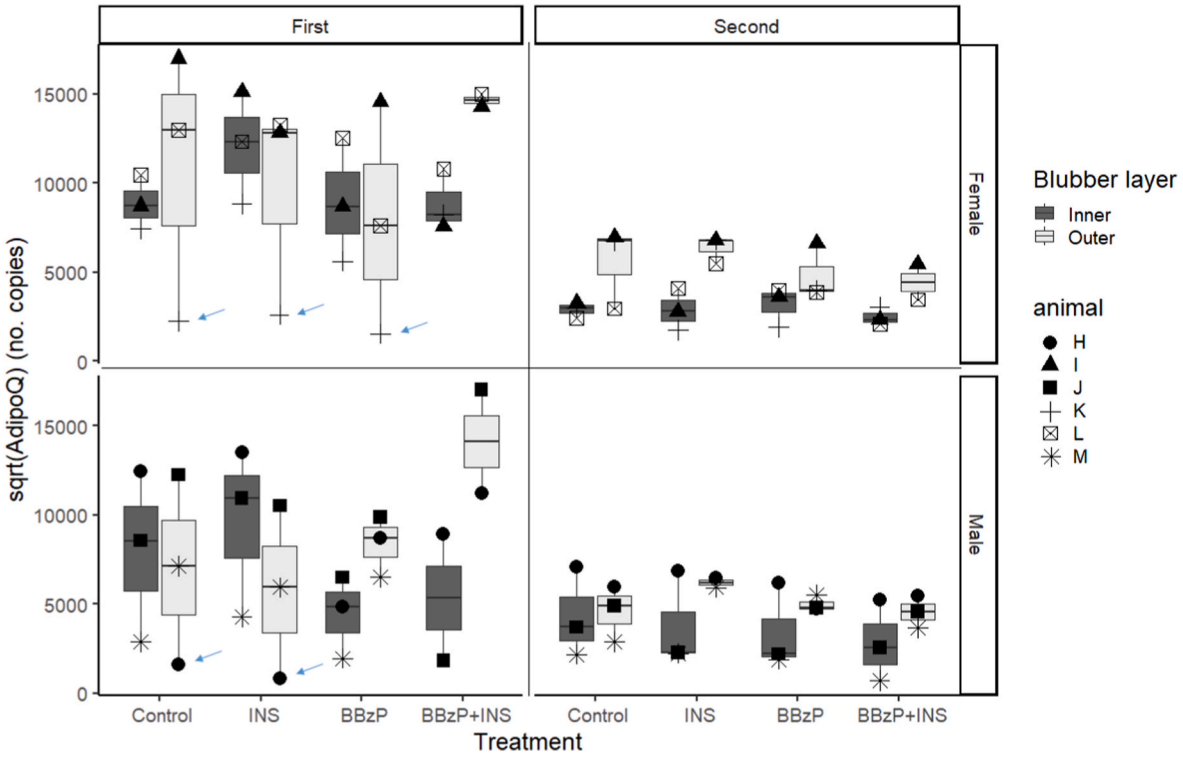

Fig. 4. sqrt (*AdipoQ*) copy number vs treatment in inner and outer tissue, on the two sampling occasions (left: first sample; right: second sample) in females (top panels) and males (bottom panels). Boxplots with upper and lower quartiles and 1.5 × interquartile range. Arrows indicate influential observations (LME: marginal R^2_{LME} = 0.33; conditional R^2_{LME} = 0.48; $n_{observations}$ = 91; $n_{animals}$ = 6).

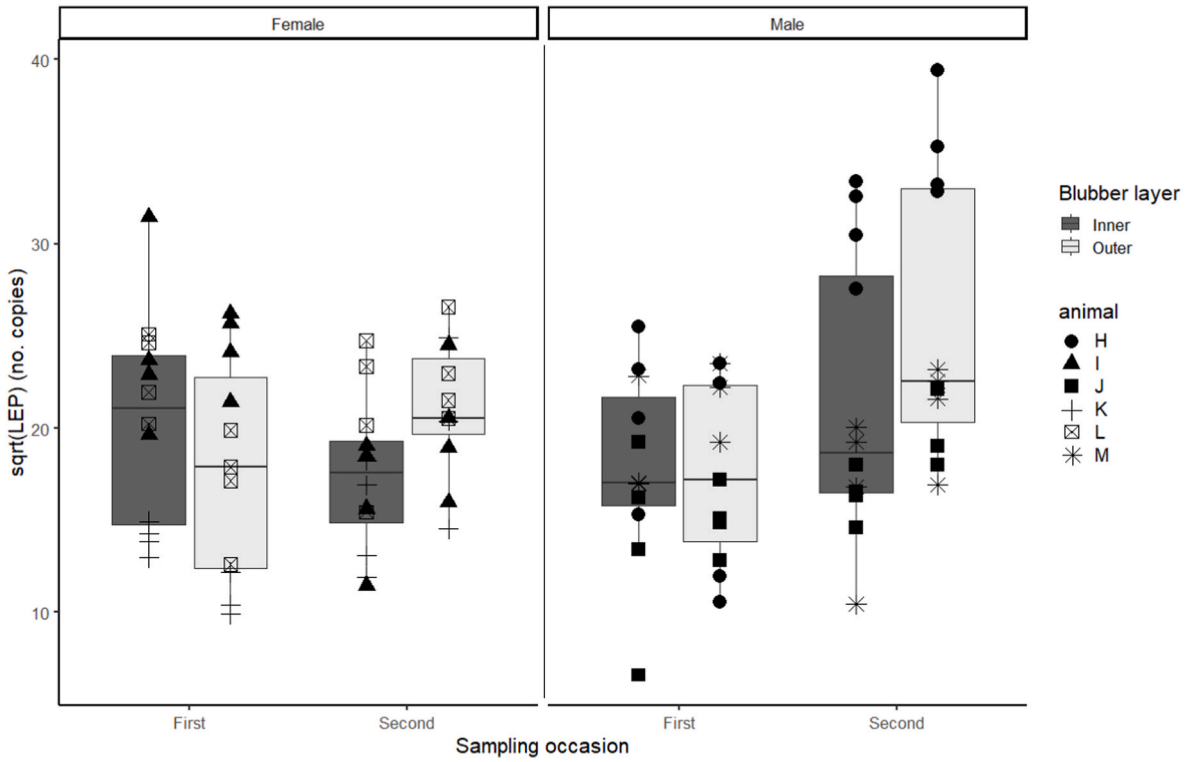

Fig. 5. Sqrt (*Lep*) copy number vs sampling occasion in females (left) and males (right). Boxplots with upper and lower quartiles and 1.5 × interquartile range. Each point represents an observation; different shapes represent different individuals ($n_{observations} = 91$; $n_{animals} = .6$).

−2.02]) and BBzP treated group (t (95) = 11.05, p < 0.001, 85% CI [−2.63, −2.02]). BBzP treatment alone did not have an effect on p-T308 (t (95) = 0.01, p = 0.992, 85% CI [−0.31, 0.30]). Combined treatment with BBzP + insulin had the same effect as insulin treatment alone (control: t (95) = 10.91, p < 0.001, 85% CI [−2.73, −2.09]; insulin treated: t (95) = 0.34, p = 0.73, 85% CI [−0.40, 0.24]; BBP treated: t (95) = 10.90, p < 0.001, 85% CI [−2.72, −2.08]) (Fig. 6E).

pAkt-T308 content was significantly higher in first compared to second sample in females (t (95) = 4.40, p < 0.001, 85% CI [0.68, 1.35]), but not in males (Fig. 6D).

5. Discussion

5.1. Effects of sample timing, mass changes and tissue depth on gene expression

Expression of genes involved in lipid metabolism changed between moulting and post-moult states, during which animals gained mass. Mass or moult-dependent differences in gene expression also differed between tissue depths. Blubber is not homogeneous throughout its depth in terms of lipid composition (Guerrero and Rogers, 2017; Tverin et al., 2019) and function (Strandberg et al., 2008; Robinson et al., 2018, 2021). Inner blubber is characterised by more dynamic lipid metabolism compared to outer (Robinson et al., 2018, 2021), which is thought to be more important for insulation (Strandberg et al., 2008). Depth variability seen here likely reflect these functional differences.

Copy number of *Pparγ,* a master regulator of transcription of metabolic genes, and *Insig2* and *Fasn,* which are involved in cholesterol and fatty acid synthesis respectively, decreased from the first to the second sampling in inner tissue, but increased in outer tissue. This suggests that lipid accumulation decreased in inner tissue, the more active part of the tissue, but increased in outer tissue as the animals gained mass. Copy number of *Scd* in both sexes and *Lep* in males also increased in outer tissue between sampling occasions, while no differences were observed in inner tissue for these two genes. These findings may suggest that during fat loss, outer tissue becomes less metabolically active while inner tissue retains its metabolic activity.

Moult or mass-specific differences in transcription were also dependent on sex, particularly *Pparg*, *Fasn* and *Lep*. This may be due to sex differences in body fat content or fuel metabolism and energy expenditure, which have previously been observed in juvenile seals (Hall and McConnell, 2007; Kelso et al., 2012), despite the lack of a clear sex difference in blubber lipid content in our small sample.

Adipoq was the only target for which a decrease between the first and the second sampling was observed in both blubber layers, regardless of sex. We cannot differentiate whether the altered gene expression patterns reflect changes in lipid metabolic processes that occurred during the last stages of the moult, or were a result of mass gain. The annual moult is a metabolically costly process, particularly in juveniles, when metabolic rate is elevated to support the cost of generating a new pelt and/or to sustain high skin temperature (Boily, 1996; Sparling et al., 2006; Paterson et al., 2012, 2021). Khudyakov et al. (2019) showed that adult female moulting northern elephant seals lost mass in late compared to early moult, and *Adipoq* transcript abundance increased with mass loss. Similarly, studies in terrestrial species show circulating adiponectin and mRNA levels negatively correlate with body fat and mass changes (Hotta et al., 2000; Ding et al., 2012). The mass gain experienced by the animals here could explain the decrease in *Adipoq* copy number in the second sample, which is also consistent with the terrestrial model. Because the animals were in captivity and fed daily, the mass gain they experienced may not reflect trajectories experienced by wild, moulting individuals that likely lose mass as a result of reduced foraging and increased metabolic costs. The data from elephant seals suggest the changes we observed are more likely to be related to mass gain than the moult per se, but this needs to be confirmed in studies in the wild.

5.2. Insulin activation of Akt

Total Akt content was higher in inner compared to outer tissue,

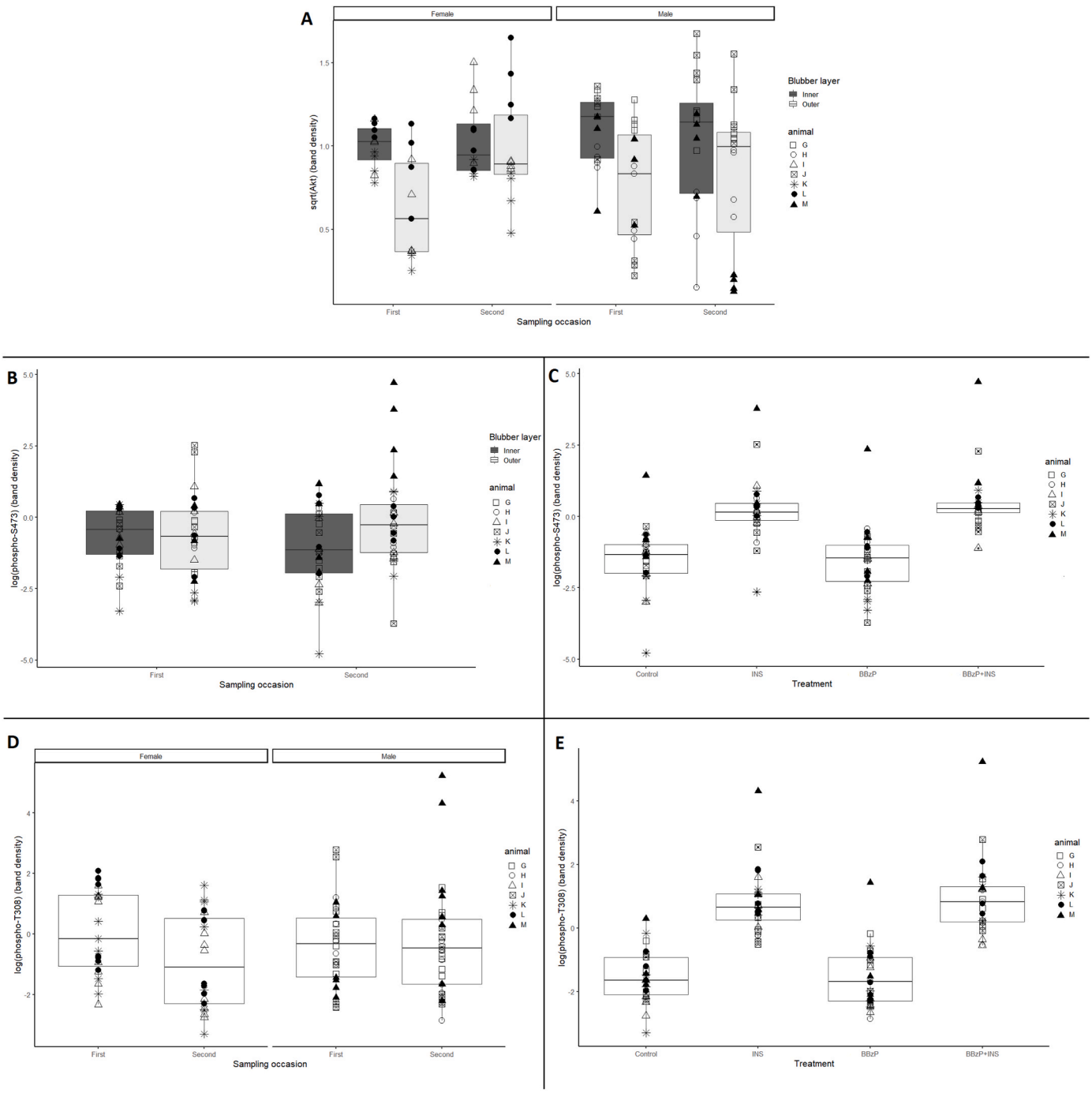

Fig. 6. (A) sqrt(Total Akt) (band density) content categorised by tissue depth. Each point shows one observation ($n_{observations} = 107$; $n\ a_{animals} = 7$). (B) log(p-S473) band density vs sampling occasion categorised by tissue depth in females (left) and males (right). Each point represents an observation ($n_{observations} = 108$; $n_{animals} = 7$). (C) log(p-S473) band density vs treatment. (D): log(p-T308) band density vs sampling occasion in females (left) and males (right). Each point shows one observation ($n_{observations} = 108$, $n_{animals} = 7$). (E) log(p-T308) band density vs treatment.

which is consistent with tissue depth differences in metabolism (Robinson et al., 2018, 2021). Insulin treatment for 30 min increased Akt phosphorylation, regardless of tissue depth and moulting status. The impact on glucose handling by the tissue was not established here due to technical limitations. In previous experiments on pups we measured glucose in media as a measure of glucose uptake (Robinson et al., 2018, 2021), but the response to insulin was too small to detect over only a 30 min exposure (Data unpublished). Additional experiments to establish whether insulin induces glucose uptake in blubber explants using fluorescent tracers would help establish the functional consequences of insulin-induced activation of Akt, particularly in light of the apparent decoupling of GLUT4 regulation from insulin signalling in other seal species (Viscarra et al., 2011b). Insulin-induced phosphorylation at the two sites shows Akt activation (Su et al., 2011), which leads to downstream stimulation of pathways involved in growth, proliferation, cell survival, and metabolism in other animals. Here, we also saw small but significant increases in *Pparγ*, *Fasn* and, in some cases, *Adipoq*, despite the short insulin exposure duration. *Fasn* is a typical insulin regulated gene (Sutherland et al. 2013; Wang and Sul, 1998) that is also regulated by PPARγ (Way et al., 2001). Insulin can induce rapid, but transient

changes in adipose-specific genes (Buyse et al., 2001; Rieusset et al., 1999). The changes we observed were small, either because the duration of exposure was too short or because downstream events from Akt, such as glycogen synthase kinase 3 (GSK-3) and mammalian target of rapamycoin (mTor) activation or forkhead box protein O1 (FOXO1) inhibition, or parallel pathways such as extracellular signal-regulated protein kinase (ERK1/2) were not strongly induced. Our results suggest that insulin can activate Akt throughout blubber depth during both the moult and post-moult stages. To confirm lack of apparent depth and moult stage or mass related differences in insulin activation of Akt and consequences for tissue function requires further work over a range of doses and including downstream proteins in the insulin signalling cascade, since here the insulin dose used may have induced maximal response and the effect of more physiological levels and on other parts of the pathway are unknown. Dose and timecourse experiments are challenging to perform in blubber explants given the limited amount of tissue available.

5.3. Impact of phthalates on blubber function

This is the first study to investigate the effects of phthalates on blubber function in pinnipeds. The effects of phthalates on marine mammal blubber remain unknown. Routti et al. (2021) showed no significant effects of DEHP or DiNP on whale PPARγ transcriptional activity, typical of earlier studies on these compounds in rat preadipocytes (Pereira-Fernandes et al., 2013, 2014). We did not explore PPARγ activation, but instead suggest its transcription may be altered by BBzP exposure, similar to previous studies on rat pre-adipocytes (Pereira-Fernandes et al., 2013, 2014; Yin et al., 2016; Sakuma et al., 2017). We found a tissue depth-specific impact of BBzP on grey seal blubber. BBzP treatment enhanced the insulin-induced *Pparγ* mRNA increase in copy number in outer tissue and suppressed it in inner tissue, while there were no significant differences in basal expression between tissue depths. There may also be an impairment in the ability of insulin to induce *Adipoq* expression. We thus show the potential for BBzP exposure to cause local metabolic disruption in seal blubber tissue. These data are consistent with the effects of BBzP and other phthalates on lipid and glucose metabolism, and insulin sensitivity in *in vitro* and *in vivo* models. 3T3-L1 pre-adipocytes exposed to BBzP show increased *Pparγ* gene expression, as well as expression of its downstream, adipocyte-specific genes, *Fasn* and *Adipoq*, during differentiation (Pereira-Fernandes et al., 2013, 2014; Yin et al., 2016; Sakuma et al., 2017). The mechanism of action of BBzP may be impacted by other local factors, such as tissue fatty acid composition, which is blubber layer dependent (Tverin et al., 2019).

Altered *Pparγ* expression could alter lipid storage and release patterns. BBzP treatment of differentiating adipocytes led to increase of *Pparγ* and other metabolic genes (including *Adipoq* and *Fasn*) (Pereira-Fernandes et al., 2013, 2014; Yin et al., 2016). In contrast, mRNA copy number of genes regulated by *Pparγ* measured here (*Scd*, *Fasn*, *Lep*), were not significantly impacted by BBzP. The lack of a change in downstream gene expression could be due to the short-term incubation and single snap shot of measurement that we were able to perform. Alternatively, seal adipocytes may be more robust to phthalate effects compared to other mammalian cultures. Further work is required to establish whether the changes observed here in response to both insulin and BBzP are transient or persistent, whether further changes in a wider suite of genes occur with longer exposure or longer time for the effects of hormone and chemical to manifest, whether PPARγ is activated in addition to its increased transcription, and what the consequences of such altered expression are for tissue function and whole animal energy storage and dynamics.

Since insulin typically acts through the activation of Akt (Sutherland et al. 2013), we examined BBzP influence on Akt phosphorylation. Overnight and longer exposures to HMW phthalates, including BBzP, alter Akt phosphorylation in other species and tissues (Chen et al., 2013; Rajesh and Balasubramanian, 2014; Deng et al., 2018; Ding et al., 2019b; Mondal and Mukherjee, 2020; Mohammadi and Ashari, 2021; Zhang and Choudhury, 2021). Here, overnight BBzP exposure had no effect on total Akt protein expression or its basal or insulin-induced phosphorylation in grey seal blubber. Our data suggest that short term exposure to BBzP does not alter canonical Akt signalling. The impact of BBzP on insulin responses at gene expression level observed here may thus be through enhanced downstream action of Akt and/or through Akt-independent pathways, such as ERK. It is also possible that altered Akt signalling occurs after longer periods of exposure (Zhang and Choudhury, 2021), but such effects could not have produced the rapid effects on gene expression seen here.

5.4. Study limitations and future directions

Phthalates occur in blubber in other marine mammals (Baini et al., 2017; Routti et al., 2021). However, there is currently no data on the presence and concentrations in UK seals, such that the consequences of our findings are hard to assess for wild populations. We used BBzP because it has a higher K_{ow} and is thus more lipophilic than lower molecular weight phthalates, and is more adipogenic in *in vitro* assays than other, more abundant, HMW phthalates (Pereira-Fernandes et al., 2013, 2014), but it is not yet clear whether this compound is of greatest concern among the phthalates for seals or what effects it may have on other lipid-rich target organs, such as the brain. While our data suggest BBzP may impact metabolic regulation, investigation of the effects of other phthalates with even higher K_{ow} values and those found consistently across marine mammal species (Routti et al., 2021; Garcia-Garin et al., 2022) and in higher concentrations in water, sediments and biota (Hidalgo-Serrano et al., 2022) is needed. The dose we used is at the lower end of that which induces adipogenesis in rat pre-adipocytes *in vitro* (Yin et al., 2016; Pereira-Fernandes et al., 2013; 2014). Dose response experiments informed by better knowledge of tissue concentrations would help to confirm the extent to which local phthalates in blubber can act as metabolic disruptors in marine mammals. It is therefore important that future research focuses on identifying the extent and nature of phthalate pollution in seals and other marine mammal species, especially given the increase in marine plastic pollution that we expect to see in the coming years (Geyer et al., 2017; Lebreton and Andrady, 2019; Borrelle et al., 2020; United Nations Environment Programme, 2021).

We focused on the expression of genes involved in lipid metabolism. The observed changes caused by BBzP treatment may not be translated at protein and functional levels. Further research is required to determine if *Pparγ* activation or increased transcription can impair appropriate lipid accumulation or mobilisation. The effect of BBzP here was observed only after a short (30 min) exposure to insulin. 'Chronic' exposure experiments are needed to investigate whether BBzP-induced disruption impacts tissue function in the longer-term. Understanding the mechanism through which BBzP alters *Pparγ* transcription and interferes with insulin signalling will help elucidate the tissue depth and moulting-status or mass dependency of BBzP-induced effects. A clearer understanding of the role of insulin in lipid deposition in seals is also required.

We were unable to disentangle the effects of moult status from mass gain because captive animals had daily access to food while in temporary captivity, in line with ethical husbandry. As a result, they gained mass when they may not typically do so in the wild at this life stage (Hall and McConnell, 2007). Further work is thus required to establish whether susceptibility to phthalate disruption is enhanced by moulting per se, or when animals are leaner.

6. Conclusion

We show here, for the first time, that the environmental pollutant, BBzP, a HMW phthalate, may induce metabolic disruption in juvenile

grey seal blubber by altering responsiveness to insulin. Our findings suggest that susceptibility to BBzP-induced disruption differs between blubber layers. In addition, we provide information on expression of adipose-specific genes during a metabolically costly process and show that differences between male and female juveniles may exist at the molecular level. The effect of BBzP in the presence of insulin, in addition to the moult or mass-specific differences in gene expression, highlight the complexity of pollutant-induced disruption and the importance of exploring metabolic disruption in different physiological states.

Author statement

KAB and AJH conceived the study and provided advice on data and sample collection and analysis; HCA, KAB and SEWM designed the study; HCA and SEWM performed field work; AT and HCA performed laboratory work; AT performed statistical analyses with advice from KAB and AJH; AT, KAB and AJH drafted the manuscript. All authors read, contributed to and approved the final draft.

Declaration of competing interest

The authors declare that they have no known competing financial interests or personal relationships that could have appeared to influence the work reported in this paper.

Data availability

These data have been submitted to the British Oceanographic Data Centre and we are awaiting a DOI

Acknowledgements

KAB, SEWM and HCA were funded by NERC grant NE/M013723/1 and AJH was funded by NE/M01357X/1 for this project. We received additional funding to AJH and KAB through the University of St Andrews from a private donor via the March Initiative and to KAB and AT at Abertay University from the Scottish Funding Council. We are grateful to NatureScot for the permit to work on the Isle of May National Nature Reserve, and Marine Scotland and the Marine Management Organisation for the permits to undertake the fieldwork. We would like to thank Mr Ryan Milne for field work and animal husbandry and Mr Matt Bivins and all the field teams involved in the logistics and collection of the samples without whom none of this work would be possible.

Appendix A. Supplementary data

Supplementary data to this article can be found online at https://doi.org/10.1016/j.envpol.2022.120688.

References

Baini, M., Martellini, T., Cincinelli, A., Campani, T., Minutoli, R., Panti, C., Finoia, M.G., Fossi, M.C., 2017. First detection of seven phthalate esters (PAEs) as plastic tracers in superficial neustonic/planktonic samples and cetacean blubber. Anal. Methods 9, 1512–1520. https://doi.org/10.1039/C6AY02674E.

Barton, K., 2018. MuMIn: Multi-Model Inference. R Package version 1.42.1. https://CRAN.R-project.org/package=MuMIn.

Bass, J.J., Wilkinson, D.J., Rankin, D., Phillips, B.E., Szewczyk, N.J., Smith, K., Atherton, P.J., 2017. An overview of technical considerations for western blotting applications to physiological research. Scand. J. Med. Sci. Sports 27, 4–25. https://doi.org/10.1111/sms.12702.

Beltifa, A., Feriani, A., Machreki, M., Ghorbel, A., Ghazouani, L., Di Bella, G., Van Loco, J., Reyns, T., Ben Mansour, H., 2017. Plasticizers and bisphenol A, in packaged foods sold in the Tunisian markets: study of their acute in vivo toxicity and their environmental fate. Environ. Sci. Pollut. Res. 24, 22382–22392. https://doi.org/10.1007/s11356-017-9861-0.

Bennett, K.A., Speakman, J.R., Moss, S.E.W., Pomeroy, P., Fedak, M.A., 2007. Effects of mass and body composition on fasting fuel utilisation in grey seal pups (*Halichoerus grypus* Fabricius): an experimental study using supplementary feeding. J. Exp. Biol. 210, 3043–3053. https://doi.org/10.1242/jeb.009381.

Bennett, K.A., Hammill, M., Currie, S., 2013. Liver glucose-6-phosphatase proteins in suckling and weaned grey seal pups: structural similarities to other mammals and relationship to nutrition, insulin signalling and metabolite levels. J. Comp. Physiol. B 183, 1075–1088. https://doi.org/10.1007/s00360-013-0768-x.

Bennett, K.A., Hughes, J., Stamatas, S., Brand, S., Foster, N.L., Moss, S.E.W., Pomeroy, P. P., 2015. Adiponectin and insulin in gray seals during suckling and fasting: relationship with nutritional state and body mass during nursing in mothers and pups. Physiol. Biochem. Zool. 88, 295–310. https://doi.org/10.1086/680862.

Bennett, K.A., Robinson, K.J., Moss, S.E.W., Millward, S., Hall, A.J., 2017. Using blubber explants to investigate adipose function in grey seals: glycolytic, lipolytic and gene expression responses to glucose and hydrocortisone. Sci. Rep. 7, 7731. https://doi.org/10.1038/s41598-017-06037-x.

Bility, M.T., 2004. Activation of mouse and human peroxisome proliferator-activated receptors (PPARs) by phthalate monoesters. Toxicol. Sci. 82, 170–182. https://doi.org/10.1093/toxsci/kfh253.

Boily, P., 1996. Metabolic and hormonal changes during the molt of captive gray seals (*Halichoerus grypus*). Am. J. Physiol. 270, R1051–R1058. https://doi.org/10.1152/ajpregu.1996.270.5.R1051.

Borrelle, S.B., Ringma, J., Law, K.L., Monnahan, C.C., Lebreton, L., McGivern, A., Murphy, E., Jambeck, J., Leonard, G.H., Hilleary, M.A., Eriksen, M., Possingham, H. P., De Frond, H., Gerber, L.R., Polidoro, B., Tahir, A., Bernard, M., Mallos, N., Barnes, M., Rochman, C.M., 2020. Predicted growth in plastic waste exceeds efforts to mitigate plastic pollution. Science 369, 1515–1518. https://doi.org/10.1126/science.aba3656.

Bustin, S., Huggett, J., 2017. qPCR primer design revisited. Biomol Detect Quant 14, 19–28. https://doi.org/10.1016/j.bdq.2017.11.001.

Buyse, M., Viengchareun, S., Bado, A., LombÈs, M., 2001. Insulin and glucocorticoids differentially regulate leptin transcription and secretion in brown adipocytes. Faseb. J. 15, 1357–1366. https://doi.org/10.1096/fj.00-0669com.

Chen, X., Qin, Q., Zhang, W., Zhang, Y., Zheng, H., Liu, C., Yang, Y., Xiong, W., Yuan, J., 2013. Activation of the PI3K–AKT–mTOR signaling pathway promotes DEHP-induced Hep3B cell proliferation. Food Chem. Toxicol. 59, 325–333. https://doi.org/10.1016/j.fct.2013.06.016.

Chiang, H., Kuo, Y.-T., Shen, C.-C., Lin, Y.-H., Wang, S.-L., Tsou, T.-C., 2016. Mono (2-ethylhexyl) phthalate accumulation disturbs energy metabolism of fat cells. Arch. Toxicol. 90, 589–601. https://doi.org/10.1007/s00204-014-1446-9.

Chomczynski, P.A., 1993. Reagent for the single-step simultaneous isolation of RNA, DNA and proteins from cell and tissue samples. Biotechniques 15 (532–4), 536–537.

Chomczynski, P., Mackey, K., 1995. Substitution of chloroform by bromochloropropane in the single-step method of RNA Isolation. Anal. Biochem. 225, 163–164. https://doi.org/10.1006/abio.1995.1126.

Daniels, P.H., 2009. A brief overview of theories of PVC plasticization and methods used to evaluate PVC-plasticizer interaction. J. Vinyl Addit. Technol. 15, 219–223. https://doi.org/10.1002/vnl.20211.

Deng, T., Zhang, Y., Wu, Y., Ma, P., Duan, J., Qin, W., Yang, X., Chen, M., 2018. Dibutyl phthalate exposure aggravates type 2 diabetes by disrupting the insulin-mediated PI3K/AKT signaling pathway. Toxicol. Lett. 290, 1–9. https://doi.org/10.1016/j.toxlet.2018.03.004.

Ding, Q., Ash, C., Mracek, T., Merry, B., Bing, C., 2012. Caloric restriction increases adiponectin expression by adipose tissue and prevents the inhibitory effect of insulin on circulating adiponectin in rats. J. Nutr. Biochem. 23, 867–874. https://doi.org/10.1016/j.jnutbio.2011.04.011.

Ding, Y., Gao, K., Liu, Y., Mao, G., Chen, K., Qiu, X., Zhao, T., Yang, L., Feng, W., Wu, X., 2019a. Transcriptome analysis revealed the mechanism of the metabolic toxicity and susceptibility of di-(2-ethylhexyl) phthalate on adolescent male ICR mice with type 2 diabetes mellitus. Arch. Toxicol. 93, 3183–3206. https://doi.org/10.1007/s00204-019-02590-8.

Ding, Y., Liu, Y., Fei, F., Yang, L., Mao, G., Zhao, T., Zhang, Z., Yan, M., Feng, W., Wu, X., 2019b. Study on the metabolism toxicity, susceptibility and mechanism of di-(2-ethylhexyl) phthalate on rat liver BRL cells with insulin resistance in vitro. Toxicology 422, 102–120. https://doi.org/10.1016/j.tox.2019.05.011.

Dziobak, M.K., Wells, R.S., Pisarski, E.C., Wirth, E.F., Hart, L.B., 2021. Demographic Assessment of Mono(2-ethylhexyl) Phthalate (MEHP) and Monoethyl Phthalate (MEP) Concentrations in Common Bottlenose Dolphins (*Tursiops truncatus*) from Sarasota Bay. FL, USA. https://doi.org/10.1029/2020GH000348. GeoHealth 5.

Dziobak, M.K., Balmer, B.C., Wells, R.S., Pisarski, E.C., Wirth, E.F., Hart, L.B., 2022. Temporal and spatial evaluation of mono(2-ethylhexyl) phthalate (MEHP) Detection in common bottlenose dolphins (*Tursiops truncatus*) from Sarasota Bay, Florida, USA. Oceans 3, 231–249. https://doi.org/10.3390/oceans3030017.

Ellero-Simatos, S., Claus, S.P., Benelli, C., Forest, C., Letourneur, F., Cagnard, N., Beaune, P.H., de Waziers, I., 2011. Combined transcriptomic– ^{1}H NMR metabonomic study reveals that monoethylhexyl phthalate stimulates adipogenesis and glyceroneogenesis in human adipocytes. J. Proteome Res. 10, 5493–5502. https://doi.org/10.1021/pr200765v.

European Food Safety Authority, EFSA CEP Panel (EFSA Panel on Food Contact Materials, Enzymes and Processing Aids), Silano, V., Barat Baviera, J.M., Bolognesi, C., Chesson, A., Cocconcelli, P.S., Crebelli, R., Gott, D.M., Grob, K., Lampi, E., Mortensen, A., Rivière, G., Steffensen, I.-L., Tlustos, C., Van Loveren, H., Vernis, L., Zorn, H., Cravedi, J.-P., Fortes, C., Tavares Poças, M.F., Waalkens-Berendsen, I., Wölfle, D., Arcella, D., Cascio, C., Castoldi, A.F., Volk, K., Castle, L., 2019. Scientific opinion on the update of the risk assessment of di-butylphthalate (DBP), butyl-benzyl-phthalate (BBP), bis(2-ethylhexyl)phthalate (DEHP), di-isononylphthalate (DINP) and di-isodecylphthalate (DIDP) for use in food contact materials. EFSA J. 17, 5838. https://doi.org/10.2903/j.efsa.2019.5838.

Feige, J.N., Gelman, L., Rossi, D., Zoete, V., Métivier, R., Tudor, C., Anghel, S.I., Grosdidier, A., Lathion, C., Engelborghs, Y., Michielin, O., Wahli, W., Desvergne, B.,

2007. The endocrine disruptor monoethyl-hexyl-phthalate is a selective peroxisome proliferator-activated receptor γ modulator that promotes adipogenesis. J. Biol. Chem. 282, 19152–19166. https://doi.org/10.1074/jbc.M702724200.

Fossi, M.C., Panti, C., Guerranti, C., Coppola, D., Giannetti, M., Marsili, L., Minutoli, R., 2012. Are baleen whales exposed to the threat of microplastics? A case study of the Mediterranean fin whale (*Balaenoptera physalus*). Mar. Pollut. Bull. 64, 2374–2379. https://doi.org/10.1016/j.marpolbul.2012.08.013.

Fossi, M.C., Coppola, D., Baini, M., Giannetti, M., Guerranti, C., Marsili, L., Panti, C., de Sabata, E., Clò, S., 2014. Large filter feeding marine organisms as indicators of microplastic in the pelagic environment: the case studies of the Mediterranean basking shark (*Cetorhinus maximus*) and fin whale (*Balaenoptera physalus*). Mar. Environ. Res. 100, 17–24. https://doi.org/10.1016/j.marenvres.2014.02.002.

Fowler, M.A., Sirpenski, G., Romano, T.A., 2020. Insulin and blubber deposition in rehabilitating harbor seal (*Phoca vitulina*) pups. Aquat. Mamm. 46, 243–253. https://doi.org/10.1578/AM.46.3.2020.243.

Fox, J., Weisberg, S., 2011. An {R} Companion to Applied Regression, second ed. Sage, Thousand Oaks CA.

Fromme, H., 2011. Phthalates: human exposure. In: Nriagu, J.O. (Ed.), Encyclopedia of Environmental Health. Elsevier, pp. 498–510. https://doi.org/10.1016/B978-0-444-52272-6.00607-3.

Garcia-Garin, O., Sahyoun, W., Net, S., Vighi, M., Aguilar, A., Ouddane, B., Víkingsson, G.A., Chosson, V., Borrell, A., 2022. Intrapopulation and temporal differences of phthalate concentrations in North Atlantic fin whales (*Balaenoptera physalus*). Chemosphere 300, 134453. https://doi.org/10.1016/j.chemosphere.2022.134453.

Geyer, R, Jameck, JR, Law, KL, 2017. Production, use, and fate of all plastics ever made. Science Advances 3 (7). https://doi.org/10.1126/sciadv.1700782.

Guerrero, A.I., Rogers, T.L., 2017. Blubber fatty acid composition and stratification in the crabeater seal, *Lobodon carcinophaga*. J. Exp. Mar. Biol. Ecol. 491, 51–57. https://doi.org/10.1016/j.jembe.2017.03.004.

Guo, W., Han, J., Wu, S., Shi, X., Wang, Q., Zhou, B., 2020. Bis(2-ethylhexyl)-2,3,4,5-tetrabromophthalate affects lipid metabolism in zebrafish larvae via DNA methylation modification. Environ. Sci. Technol. 54, 355–363. https://doi.org/10.1021/acs.est.9b05796.

Hall, A.J., McConnell, B.J., 2007. Measuring changes in juvenile gray seal body composition. Mar. Mamm. Sci. 23, 650–665. https://doi.org/10.1111/j.1748-7692.2007.00132.x.

Hall, A.J., McConnell, B.J., Barker, R.J., 2002. The effect of total immunoglobulin levels, mass and condition on the first-year survival of grey seal pups. Funct. Ecol. 16, 462–474. https://doi.org/10.1046/j.1365-2435.2002.00649.x.

Harris, C.A., Henttu, P., Parker, M.G., Sumpter, J.P., 1997. The estrogenic activity of phthalate esters *in vitro*. Environ. Health Perspect. 105, 802–811. https://doi.org/10.2307/3433697.

Hart, L.B., Dziobak, M.K., Pisarski, E.C., Wirth, E.F., Wells, R.S., 2020. Sentinels of synthetics – a comparison of phthalate exposure between common bottlenose dolphins (*Tursiops truncatus*) and human reference populations. PLoS One 15, e0240506. https://doi.org/10.1371/journal.pone.0240506.

Hidalgo-Serrano, M., Borrull, F., Marcé, R.M., Pocurull, E., 2022. Phthalate esters in marine ecosystems: analytical methods, occurrence and distribution. Trends Anal. Chem. 151, 116598 https://doi.org/10.1016/j.trac.2022.116598.

Hotta, K., Funahashi, T., Arita, Y., Takahashi, M., Matsuda, M., Okamoto, Y., Iwahashi, H., Kuriyama, H., Ouchi, N., Maeda, K., Nishida, M., Kihara, S., Sakai, N., Nakajima, T., Hasegawa, K., Muraguchi, M., Ohmoto, Y., Nakamura, T., Yamashita, S., Hanafusa, T., Matsuzawa, Y., 2000. Plasma concentrations of a novel, adipose-specific protein, adiponectin, in type 2 diabetic patients. ATVB 20, 1595–1599. https://doi.org/10.1161/01.ATV.20.6.1595.

Houser, D.S., Champagne, C.D., Crocker, D.E., 2013. A non-traditional model of the metabolic syndrome: the adaptive significance of insulin resistance in fasting-adapted seals. Front. Endocrinol. 4 https://doi.org/10.3389/fendo.2013.00164.

Hurst, C.H., Waxman, D.J., 2003. Activation of PPAR and PPAR by environmental phthalate monoesters. Toxicol. Sci. 74, 297–308. https://doi.org/10.1093/toxsci/kfg145.

Irving, L., Hart, J.S., 1957. The metabolism and insulation of seals as are-skinned mammals in cold water. Can. J. Zool. 35, 497–511. https://doi.org/10.1139/z57-041.

Jambeck, J.R., Geyer, R., Wilcox, C., Siegler, T.R., Perryman, M., Andrady, A., Narayan, R., Law, K.L., 2015. Plastic waste inputs from land into the ocean. Science 347, 768–771. https://doi.org/10.1126/science.1260352.

Janjua, N.R., Frederiksen, H., Skakkebæk, N.E., Wulf, H.C., Andersson, A.-M., 2008. Urinary excretion of phthalates and paraben after repeated whole-body topical application in humans. Int. J. Androl. 31, 118–130. https://doi.org/10.1111/j.1365-2605.2007.00841.x.

Jia, Y., Liu, T., Zhou, L., Zhu, J., Wu, J., Sun, D., Xu, J., Wang, Q., Chen, H., Xu, F., Zhang, Y., Zhang, T., Liu, H., Ye, L., 2016. Effects of di-(2-ethylhexyl) phthalate on lipid metabolism by the JAK/STAT pathway in rats. IJERPH 13, 1085. https://doi.org/10.3390/ijerph13111085.

Kastner, J., Cooper, D.G., Marić, M., Dodd, P., Yargeau, V., 2012. Aqueous leaching of di-2-ethylhexyl phthalate and "green" plasticizers from poly(vinyl chloride). Sci. Total Environ. 432, 357–364. https://doi.org/10.1016/j.scitotenv.2012.06.014.

Kelso, E.J., Champagne, C.D., Tift, M.S., Houser, D.S., Crocker, D.E., 2012. Sex differences in fuel use and metabolism during development in fasting juvenile northern elephant seals. J. Exp. Biol. 215, 2637–2645. https://doi.org/10.1242/jeb.068833.

Khudyakov, J.I., Abdollahi, E., Ngo, A., Sandhu, G., Stephan, A., Costa, D.P., Crocker, D. E., 2019. Expression of obesity-related adipokine genes during fasting in a naturally obese marine mammal. Am. J. Physiol. 317, R521–R529. https://doi.org/10.1152/ajpregu.00182.2019.

Koch, H.M., Lorber, M., Christensen, K.L.Y., Pälmke, C., Koslitz, S., Brüning, T., 2013. Identifying sources of phthalate exposure with human biomonitoring: results of a 48h fasting study with urine collection and personal activity patterns. Int. J. Hyg Environ. Health 216, 672–681. https://doi.org/10.1016/j.ijheh.2012.12.002.

Koch, H.M., Rüther, M., Schütze, A., Conrad, A., Pälmke, C., Apel, P., Brüning, T., Kolossa-Gehring, M., 2017. Phthalate metabolites in 24-h urine samples of the German Environmental Specimen Bank (ESB) from 1988 to 2015 and a comparison with US NHANES data from 1999 to 2012. Int. J. Hyg Environ. Health 220, 130–141. https://doi.org/10.1016/j.ijheh.2016.11.003.

Koressaar, T., Remm, M., 2007. Enhancements and modifications of primer design program Primer3. Bioinformatics 23, 1289–1291. https://doi.org/10.1093/bioinformatics/btm091.

Landrigan, P.J., Stegeman, J.J., Fleming, L.E., Allemand, D., Anderson, D.M., Backer, L. C., Brucker-Davis, F., Chevalier, N., Corra, L., Czerucka, D., Bottein, M.-Y.D., Demeneix, B., Depledge, M., Deheyn, D.D., Dorman, C.J., Fénichel, P., Fisher, S., Gaill, F., Galgani, F., Gaze, W.H., Giuliano, L., Grandjean, P., Hahn, M.E., Hamdoun, A., Hess, P., Judson, B., Laborde, A., McGlade, J., Mu, J., Mustapha, A., Neira, M., Noble, R.T., Pedrotti, M.L., Reddy, C., Rocklöv, J., Scharler, U.M., Shanmugam, H., Taghian, G., Van de Water, J.A.J.M., Vezzulli, L., Weihe, P., Zeka, A., Raps, H., Rampal, P., 2020. Human health and ocean pollution. Annal Global Health 86, 151. https://doi.org/10.5334/aogh.2831.

Lau, W.W.Y., Shiran, Y., Bailey, R.M., Cook, E., Stuchtey, M.R., Koskella, J., Velis, C.A., Godfrey, L., Boucher, J., Murphy, M.B., Thompson, R.C., Jankowska, E., Castillo Castillo, A., Pilditch, T.D., Dixon, B., Koerselman, L., Kosior, E., Favoino, E., Gutberlet, J., Baulch, S., Atreya, M.E., Fischer, D., He, K.K., Petit, M.M., Sumaila, U. R., Neil, E., Bernhofen, M.V., Lawrence, K., Palardy, J.E., 2020. Evaluating scenarios toward zero plastic pollution. Science 369, 1455–1461. https://doi.org/10.1126/science.aba9475.

Lebreton, L., Andrady, A., 2019. Future scenarios of global plastic waste generation and disposal. Palgrave Commun 5, 6. https://doi.org/10.1057/s41599-018-0212-7.

Lefcheck, J.S., 2016. piecewiseSEM: piecewise structural equation modelling in R for ecology, evolution, and systematics. Methods Ecol. Evol. 7, 573–579. https://doi.org/10.1111/2041-210X.12512.

Leong, D.T., Gupta, A., Bai, H.F., Wan, G., Yoong, L.F., Too, H.-P., Chew, F.T., Hutmacher, D.W., 2007. Absolute quantification of gene expression in biomaterials research using real-time PCR. Biomaterials 28, 203–210. https://doi.org/10.1016/j.biomaterials.2006.09.011.

Lidgard, D.C., Boness, D.J., Bowen, W.D., McMillan, J.I., 2005. State-dependent male mating tactics in the grey seal: the importance of body size. Behav. Ecol. 16, 541–549. https://doi.org/10.1093/beheco/ari023.

Mackintosh, C.E., Maldonado, J., Hongwu, J., Hoover, N., Chong, A., Ikonomou, M.G., Gobas, F.A.P.C., 2004. Distribution of phthalate esters in a marine aquatic food Web: comparison to polychlorinated biphenyls. Environ. Sci. Technol. 38, 2011–2020. https://doi.org/10.1021/es034745r.

Merck, 2022. TRI Reagent protocol. Available at: https://www.sigmaaldrich.com/GB/en/technical-documents/protocol/protein-biology/protein-lysis-and-extraction/tri-reagent. (Accessed 14 October 2022). Accessed.

Mes, J., Coffin, D.E., Campbell, D.S., 1974. Di-n-butyl-and Di-2-ethylhexyl phthalate in human adipose tissue. Bull. Environ. Contam. Toxicol. 12, 721–725. https://doi.org/10.1007/BF01685921.

Mohammadi, H., Ashari, S., 2021. Mechanistic insight into toxicity of phthalates, the involved receptors, and the role of Nrf2, NF-κB, and PI3K/AKT signaling pathways. Environ. Sci. Pollut. Res. 28, 35488–35527. https://doi.org/10.1007/s11356-021-14466-5.

Mondal, S., Mukherjee, S., 2020. Long-term dietary administration of diethyl phthalate triggers loss of insulin sensitivity in two key insulin target tissues of mice. Hum. Exp. Toxicol. 39, 984–993. https://doi.org/10.1177/0960327120909526.

Montoto-Martínez, T., De la Fuente, J., Puig-Lozano, R., Marques, N., Arbelo, M., Hernández-Brito, J.J., Fernández, A., Gelado-Caballero, M.D., 2021. Microplastics, bisphenols, phthalates and pesticides in odontocete species in the macronesian region (eastern north atlantic). Mar. Pollut. Bull. 173, 113105 https://doi.org/10.1016/j.marpolbul.2021.113105.

Moody, L., Hernández-Saavedra, D., Kougias, D.G., Chen, H., Juraska, J.M., Pan, Y.-X., 2019a. Tissue-specific changes in Srebf1 and Srebf2 expression and DNA methylation with perinatal phthalate exposure. Environmental Epigenetics 5, dvz009. https://doi.org/10.1093/eep/dvz009.

Moody, L., Kougias, D., Jung, P.M., Digan, I., Hong, A., Gorski, A., Chen, H., Juraska, J., Pan, Y.-X., 2019b. Perinatal phthalate and high-fat diet exposure induce sex-specific changes in adipocyte size and DNA methylation. J. Nutr. Biochem. 65, 15–25. https://doi.org/10.1016/j.jnutbio.2018.11.005.

Navarro, R., Pérez Perrino, M., Gómez Tardajos, M., Reinecke, H., 2010. Phthalate plasticizers covalently bound to PVC: plasticization with suppressed migration. Macromolecules 43, 2377–2381. https://doi.org/10.1021/ma902740t.

Nelms, S.E., Galloway, T.S., Godley, B.J., Jarvis, D.S., Lindeque, P.K., 2018. Investigating microplastic trophic transfer in marine top predators. Environ. Pol. 238, 999–1007. https://doi.org/10.1016/j.envpol.2018.02.016.

Nelms, S.E., Barnett, J., Brownlow, A., Davison, N.J., Deaville, R., Galloway, T.S., Lindeque, P.K., Santillo, D., Godley, B.J., 2019. Microplastics in marine mammals stranded around the British coast: ubiquitous but transitory? Sci. Rep. 9, 1075. https://doi.org/10.1038/s41598-018-37428-3.

Olmstead, K.I., La Frano, M.R., Fahrmann, J., Grapov, D., Viscarra, J.A., Newman, J.W., Fiehn, O., Crocker, D.E., Filipp, F.V., Ortiz, R.M., 2017. Insulin induces a shift in lipid and primary carbon metabolites in a model of fasting-induced insulin resistance. Metabolomics 13, 60. https://doi.org/10.1007/s11306-017-1186-y.

Omowunmi, H.F.-.A., Ayejuyo, O.O., Benson, N.U., 2020. Dataset on microplastics and associated trace metals and phthalate esters in sandy beaches of tropical Atlantic ecosystems, Nigeria. Data Brief 31, 105755. https://doi.org/10.1016/j.dib.2020.105755.

Paluselli, A., Fauvelle, V., Galgani, F., Sempere, R., 2019. Phthalate release from plastic fragments and degradation in seawater. Environ. Sci. Technol. 53, 166–175. https://doi.org/10.1021/acs.est.8b05083.

Paterson, W., Sparling, C.E., Thompson, D., Pomeroy, P.P., Currie, J.I., McCafferty, D.J., 2012. Seals like it hot: changes in surface temperature of harbour seals (*Phoca vitulina*) from late pregnancy to moult. J. Therm. Biol. 37, 454–461. https://doi.org/10.1016/j.jtherbio.2012.03.004.

Paterson, W.D., Moss, S.E., Milne, R., Currie, J.I., McCafferty, D.J., Thompson, D., 2021. Increased metabolic rate of hauled-out harbor seals (*Phoca vitulina*) during the molt. Physiol. Biochem. Zool. 94, 152–161. https://doi.org/10.1086/713958.

Pereira-Fernandes, A., Demaegdt, H., Vandermeiren, K., Hectors, T.L., Jorens, P.G., Blust, R., Vanparys, C., 2013. Evaluation of a screening system for obesogenic compounds: screening of endocrine disrupting compounds and evaluation of the PPAR dependency of the effect. PLoS One 8, e77481. https://doi.org/10.1371/journal.pone.0077481.

Pereira-Fernandes, A., Vanparys, C., Vergauwen, L., Knapen, D., Joren, s P.G., Blust, R., 2014. Toxicogenomics in the 3T3-L1 cell line, a new approach for screening of obesogenic compounds. Toxicol. Sci. 14, 352–363. https://doi.org/10.1093/toxsci/kfu092.

Persico, P., Ambrogi, V., Acierno, D., Carfagna, C., 2009. Processability and mechanical properties of commercial PVC plastisols containing low-environmental-impact plasticizers. J. Vinyl Addit. Technol. 15, 139–146. https://doi.org/10.1002/vnl.20187.

Persson, L., Carney Almroth, B.M., Collins, C.D., Cornell, S., de Wit, C.A., Diamond, M.L., Fantke, P., Hassellöv, M., MacLeod, M., Ryberg, M.W., Søgaard Jørgensen, P., Villarrubia-Gómez, P., Wang, Z., Hauschild, M.Z., 2022. Outside the safe operating space of the planetary boundary for novel entities. Environ. Sci. Technol. 56, 1510–1521. https://doi.org/10.1021/acs.est.1c04158.

Pinheiro, J., Bates, D., DebRoy, S., Sarkar, D., R Core Team, 2018. Nlme: Linear and Nonlinear Mixed Effects Models_. R Package Version 3.1-137. URL: https://CRAN.R-project.org/package=nlme.

Plastics Europe, 2021. Plastics: the facts. Available at: https://plasticseurope.org/knowledge-hub/plastics-the-facts-2021/. Accessed 20.20.2022.

Pomeroy, P.P., Fedak, M.A., Rothery, P., Anderson, S., 1999. Consequences of maternal size for reproductive expenditure and pupping success of grey seals at North Rona, Scotland. J. Anim. Ecol. 68, 235–253. https://doi.org/10.1046/j.1365-2656.1999.00281.x.

Radke, E.G., Galizia, A., Thayer, K.A., Cooper, G.S., 2019. Phthalate exposure and metabolic effects: a systematic review of the human epidemiological evidence. Environ. Int. 132, 104768 https://doi.org/10.1016/j.envint.2019.04.040.

Rajesh, P., Balasubramanian, K., 2014. Phthalate exposure in utero causes epigenetic changes and impairs insulin signalling. J. Endocrinol. 223, 47–66. https://doi.org/10.1530/JOE-14-0111.

Reilly, J.J., 1991. Adaptations to prolonged fasting in free-living weaned gray seal pups. Am. J. Physiol. 260, R267–R272. https://doi.org/10.1152/ajpregu.1991.260.2.R267.

Rian, M.B., Vike-Jonas, K., Gonzalez, S.V., Ciesielski, T.M., Venkatraman, V., Lindstrøm, U., Jenssen, B.M., Asimakopoulos, A.G., 2020. Phthalate metabolites in harbor porpoises (*Phocoena phocoena*) from Norwegian coastal waters. Environ. Int. 137, 105525 https://doi.org/10.1016/j.envint.2020.105525.

Rieusset, J., Andreelli, F., Auboeuf, D., Roques, M., Vallier, P., Riou, J.P., Auwerx, J., Laville, M., Vidal, H., 1999. Insulin acutely regulates the expression of the peroxisome proliferator-activated receptor-gamma in human adipocytes. Diabetes 48, 699–705. https://doi.org/10.2337/diabetes.48.4.699.

Robinson, K.J., Hall, A.J., Debier, C., Eppe, G., Thomé, J.-P., Bennett, K.A., 2018. Persistent organic pollutant burden, experimental POP exposure, and tissue properties affect metabolic profiles of blubber from gray seal pups. Environ. Sci. Technol. 52, 13523–13534. https://doi.org/10.1021/acs.est.8b04240.

Robinson, K.J., Hall, A.J., Scholl, G., Debier, C., Thomé, J., Eppe, G., Adam, C., Bennett, K.A., 2019. Investigating decadal changes in persistent organic pollutants in Scottish grey seal pups. Aquat. Conserv. Mar. Freshw. Ecosyst. 29, 86–100. https://doi.org/10.1002/aqc.3137.

Robinson, K.J., Armstrong, H.C., Moss, S.E.W., Oller, L., Hall, A.J., Bennett, K.A., 2021. Signs of life: oxygen sensors confirm viability, measure oxygen consumption and provide rapid, effective contamination monitoring for field-based tissue culture. Methods Ecol. Evol. 12, 2410–2420. https://doi.org/10.1111/2041-210X.13710.

Routti, H., Harju, M., Lühmann, K., Aars, J., Ask, A., Goksøyr, A., Kovacs, K.M., Lydersen, C., 2021. Concentrations and endocrine disruptive potential of phthalates in marine mammals from the Norwegian Arctic. Environ. Int. 152, 106458 https://doi.org/10.1016/j.envint.2021.106458.

Sakuma, S., Sumida, M., Endoh, Y., Kurita, A., Yamaguchi, A., Watanabe, T., Kohda, T., Tsukiyama, Y., Fujimoto, Y., 2017. Curcumin inhibits adipogenesis induced by benzyl butyl phthalate in 3T3-L1 cells. Toxicol. Appl. Pharmacol. 329, 158–164. https://doi.org/10.1016/j.taap.2017.05.036.

Senko, J., Nelms, S., Reavis, J., Witherington, B., Godley, B., Wallace, B., 2020. Understanding individual and population-level effects of plastic pollution on marine megafauna. Endanger. Species Res. 43, 234–252. https://doi.org/10.3354/esr01064.

Sparling, C.E., Speakman, J.R., Fedak, M.A., 2006. Seasonal variation in the metabolic rate and body composition of female grey seals: fat conservation prior to high-cost reproduction in a capital breeder? J. Comp. Physiol. B 176, 505–512. https://doi.org/10.1007/s00360-006-0072-0.

Strandberg, U., Käkelä, A., Lydersen, C., Kovacs, K.M., Grahl-Nielsen, O., Hyvärinen, H., Käkelä, R., 2008. Stratification, composition, and function of marine mammal blubber: the ecology of fatty acids in marine mammals. Physiol. Biochem. Zool. 81, 473–485. https://doi.org/10.1086/589108.

Su, C.-H., Wang, C.-Y., Lan, K.-H., Li, C.-P., Chao, Y., Lin, H.-C., Lee, S.-D., Lee, W.-P., 2011. Akt phosphorylation at Thr308 and Ser473 is required for CHIP-mediated ubiquitination of the kinase. Cell. Signal. 23, 1824–1830. https://doi.org/10.1016/j.cellsig.2011.06.018.

Sutherland, C, O'Brien, RM, Granner, DK, 2013. Insulin Action Gene Regulation. In Madame Curie Bioscience Database [Internet]. Austin (TX): Landes Bioscience; 2000-2013. https://www.ncbi.nlm.nih.gov/books/NBK6471/#_NBK6471_pubdet_.

Thermofisher.com, 2016a. Invitrogen user guide. SYBR™ safe DNA gel stain. Available at: https://www.thermofisher.com/document-connect/document-connect.html?url=https://assets.thermofisher.com/TFS-Assets%2FLSG%2Fmanuals%2Fsybr_safe_dna_gel_stain_man.pdf. (Accessed 14 October 2022). Accessed.

Thermofisher.com, 2016b. Invitrogen user guide. Pierce™ BCA protein assay kit. https://www.thermofisher.com/document-connect/document-connect.html?url=https://assets.thermofisher.com/TFS-Assets%2FLSG%2Fmanuals%2FMAN0011430_Pierce_BCA_Protein_Asy_UG.pdf. (Accessed 14 October 2022). Accessed.

Tverin, M., Westberg, M., Kokkonen, I., Tang, P., Lehmann, P., Lundström, K., Käkelä, R., 2019. Factors affecting the degree of vertical stratification of fatty acids in grey seal blubber. Mar. Biol. 166, 105. https://doi.org/10.1007/s00227-019-3556-7.

United Nations Environment Programme, 2021. From Pollution to Solution: A Global Assessment of Marine Litter and Plastic Pollution. Nairobi. Available at: https://www.unep.org/resources/pollution-solution-global-assessment-marine-litter-and-plastic-pollution. (Accessed 10 February 2022). accessed.

Untergasser, A., Cutcutache, I., Koressaar, T., Ye, J., Faircloth, B.C., Remm, M., Rozen, S.G., 2012. Primer3–new capabilities and interfaces. Nucleic Acids Res. 40, e115. https://doi.org/10.1093/nar/gks596.

van der Meer, T.P., van Faassen, M., van Beek, A.P., Snieder, H., Kema, I.P., Wolffenbuttel, B.H.R., van Vliet-Ostaptchouk, J.V., 2020. Exposure to endocrine disrupting chemicals in the Dutch general population is associated with adiposity-related traits. Sci. Rep. 10, 9311. https://doi.org/10.1038/s41598-020-66284-3.

Viscarra, J.A., Champagne, C.D., Crocker, D.E., Ortiz, R.M., 2011a. 5′AMP-activated protein kinase activity is increased in adipose tissue of northern elephant seal pups during prolonged fasting-induced insulin resistance. J. Endocrinol. 209, 317–325. https://doi.org/10.1530/JOE-11-0017.

Viscarra, J.A., Vázquez-Medina, J.P., Crocker, D.E., Ortiz, R.M., 2011b. Glut4 is upregulated despite decreased insulin signaling during prolonged fasting in northern elephant seal pups. Am. J. Physiol. 300, R150. https://doi.org/10.1152/ajpregu.00478.2010. –R154.

Wang, LY, Gu, YY, Zhang, ZM, Sun, AL, Shi, XZ, Chen, J, Lu, Y, 2021. Contaminant occurrence, mobility and ecological risk assessment of phthalate esters in the sediment-water system of the Hangzhou Bay. Science of the Total Environment 770, 144705. https://doi.org/10.1016/j.scitotenv.2020.144705. https://www.sciencedirect.com/science/article/pii/S0048969720382383.

Wang, D., Sul, H.S., 1998. Insulin stimulation of the fatty acid synthase promoter Is mediated by the phosphatidylinositol 3-kinase pathway. J. Biol. Chem. 273, 25420–25426. https://doi.org/10.1074/jbc.273.39.25420.

Way, J.M., Harrington, W.W., Brown, K.K., Gottschalk, W.K., Sundseth, S.S., Mansfield, T.A., Ramachandran, R.K., Willson, T.M., Kliewer, S.A., 2001. Comprehensive messenger ribonucleic acid profiling reveals that peroxisome proliferator-activated receptor γ activation has coordinate effects on gene expression in multiple insulin-sensitive tissues. Endocrinology 142, 1269–1277. https://doi.org/10.1210/endo.142.3.8037.

World Health Organization & International Programme on Chemical Safety, 1999. Butyl Benzyl Phthalate. World Health Organization. https://apps.who.int/iris/handle/10665/42201.

Xiong, J., Yang, Q., Kang, J., Sun, Y., Zhang, T., Margaret, G., Ding, W., 2011. Simultaneous isolation of DNA, RNA, and protein from *Medicago truncatula* L. Electrophoresis 32, 321–330. https://doi.org/10.1002/elps.201000425.

Yin, L., Yu, K.S., Lu, K., Yu, X., 2016. Benzyl butyl phthalate promotes adipogenesis in 3T3-L1 preadipocytes: a high content cellomics and metabolomic analysis. Toxicol. Vitro 32, 297–309. https://doi.org/10.1016/j.tiv.2016.01.010.

Zhang, J., Choudhury, M., 2021. Benzyl butyl phthalate induced early lncRNA H19 regulation in C3H10T1/2 stem cell line. Chem. Res. Toxicol. 34, 54–62. https://doi.org/10.1021/acs.chemrestox.0c00129.

Zhang, H., Ben, Y., Han, Y., Zhang, Y., Li, Y., Chen, X., 2022. Phthalate exposure and risk of diabetes mellitus: implications from a systematic review and meta-analysis. Environ. Res. 204, 112109 https://doi.org/10.1016/j.envres.2021.112109.

Zuur, A.F., Ieno, E.N., Elphick, C.S., 2010. A protocol for data exploration to avoid common statistical problems: data exploration. Methods Ecol. Evol. 1, 3–14. https://doi.org/10.1111/j.2041-210X.2009.00001.x.